Sustainable Cities and Society 116 (2024) 105907

Contents lists available at ScienceDirect

Sustainable Cities and Society

journal homepage: www.elsevier.com/locate/scs

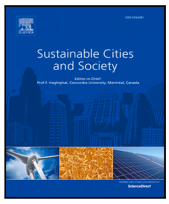

Projected risk and vulnerability to heat waves for Montreal, Quebec, using Gaussian processes

Jean-Nicolas Côté [a,*], Elisabeth Levac [b], Mickaël Germain [a], Eric Lavigne [c,d]

[a] Department of Applied Geomatics, Université de Sherbrooke, 2500, boulevard de l'Université, Sherbrooke, Quebec, J1K 2R1, Canada
[b] Department of Environment, Agriculture and Geography, Bishop's University, 2600 College St., Sherbrooke, Quebec, J1M 1Z7, Canada
[c] Environmental Health Science and Research Bureau, Health Canada, Ottawa, Ontario, Canada
[d] School of Epidemiology & Public Health, University of Ottawa, Ottawa, Ontario, Canada

ARTICLE INFO

Keywords:
Climate change
Public health
Adaptation
Geographic information system
Machine learning
Shared socioeconomic pathways

ABSTRACT

Urban areas face increasing climate risks and are at the forefront of adaptation challenges. Despite the growing number of cities that are developing adaptation plans, they often fail to implement, monitor, and evaluate them. This article addresses this issue by modelling a comprehensive risk assessment that includes vulnerability using Gaussian processes. Mortality during heat waves for the City of Montreal, Quebec, is used as a case study. The vulnerability model includes sensitivity components (age and socioeconomic variables) and an adaptive capacity component (a suitable level of vegetation to decrease the urban heat island effect). Various aging and climate scenarios (SSP1-2.6, SSP2-4.5 and SSP5-8.5) are used for projections up to year 2100. SHAP values are used to show features contributions to the model. As the climate warms, Montreal will face increasing summer mortality. The city should therefore increase its vegetation cover in vulnerable neighbourhoods. Despite inherent limitations to the complexity of risk modelling, this approach facilitates the implementation of adaptation solutions and their monitoring. Greater effort should be made in the future to improve comprehensive risk modelling and more research is required to validate which framework is best in closing the gap between science and political decisions.

1. Introduction

Chapter 6 *Cities, Settlements and Key Infrastructure* of the Working Group (WG) II contributing to the Sixth Assessment Report (AR6) of the Intergovernmental Panel on Climate Change (IPCC) concluded that urban areas face increasing climate risks and, therefore, are at the forefront of adaptation challenges. They also noted that despite the growing number of cities that are developing adaptation plans, their subsequent implementation, monitoring, and evaluation is lacking (Dodman et al., 2022). One possible explanation for these shortcomings is the absence of a validation process in most vulnerability frameworks that are essential to adaptation plans. A systematic review by Cheng et al. (2021) highlighted that only 26.9% of the articles reviewed on heat-vulnerable populations had a validation process. Another systematic review on social vulnerability indices (SVIs) for various natural hazards by Painter, et al. (2024) had a similar finding, noting that 76% of the articles reviewed did not have any validation process. Both articles also highlighted the absence of gold standards in the validation process, making it very hard to properly compare two different frameworks. Therefore, the high number of SVIs available in the literature are not necessarily of high quality, and more frameworks with a strong validation process are needed (Karanja & Kiage, 2021; Kuhlicke, et al., 2023; Li et al., 2024).

Beyond the lack of validation, SVIs are usually built with principal component analysis (PCA) (Li et al., 2022), leading to other problems. The difficulty in interpreting PCA scores to guide decision making (Li et al., 2022; Sheehan et al., 2023; Spielman et al., 2020), the lack of correlation between PCA scores and climate impacts (Goodman et al., 2021), and the lack of agreement between studies that are based on expert opinions (Garschagen et al., 2021; Raška et al., 2020) are a few reasons why SVIs might not be the best choice to assess vulnerability.

There are obviously also high-quality articles that have a validation process for exposure (Liu et al., 2024; Sützl et al., 2024), specific outcome (Boudreault et al., 2024b; Singh et al., 2024) or vulnerability index (Seong et al., 2024; Wang et al., 2024). These articles are helpful and we encourage more researchers to integrate a proper validation process before publishing. Yet, their narrow scope focusing only on a fraction of a comprehensive risk assessment based on the IPCC

* Corresponding author.
E-mail address: jean-nicolas.cote@usherbrooke.ca (J.-N. Côté).

https://doi.org/10.1016/j.scs.2024.105907
Received 29 July 2024; Received in revised form 4 October 2024; Accepted 14 October 2024
Available online 28 October 2024

definition makes it difficult for practitioners to have a complete picture of the situation.

In trying to address this issue, we previously developed a data-driven framework that covers every step of a climate risk analysis, including a vulnerability assessment (Côté et al., 2024). Our article provided the theoretical foundations for a framework that is based on WG II contributions to the AR6 (Pörtner et al., 2022). We further explained how to use it, but did not provide examples that include various climate projections.

The observations about vulnerability and risk frameworks in this introduction raise the question : Is it possible to have a unique framework with a strong validation process for the risk and vulnerability assessment, including climate projections, to improve decision making for adaptation options? To the best of our knowledge, no article has attempted this before.

This article tries to bridge this gap by presenting a case study demonstrating how to perform a complete risk assessment that includes aging and climate projection scenarios for Montreal, Quebec (Canada). While this kind of projection is found in the literature (Wan et al., 2024; Weber et al., 2023), it usually does not include a comprehensive risk assessment with a vulnerability component that incorporates multiple socioeconomic and environmental variables, as does our study.

We briefly summarize the methodology of our previous article (see the flowchart in Appendix A) (Côté et al., 2024). The focal point of this risk framework is the selection of the best adaptation options to reduce the impacts of a hazard. Given that the magnitude of the impact is not usually homogeneous in the exposed region, a vulnerability assessment is required to prioritize the most vulnerable locations. Following this logic, in the present article, we model the increase in historical daily mortality rates during heat waves for the City of Montreal. The vulnerability assessment reveals different mortality rates among neighbourhoods. The vulnerability model includes sensitivity components (age and socioeconomic variables) and an adaptive capacity component (a suitable level of vegetation to decrease the urban heat island effect). We also project impacts that are based on different aging and climate scenarios based on shared socioeconomic pathways (SSP1-2.6, SSP2-4.5, SSP5-5.8). All of this information is crucial for policymakers in selecting the best adaptation options. It also highlights the importance of better mitigation measures to reduce greenhouse gases (GHGs).

Our previous results evaluating different artificial intelligence (AI) and machine-learning (ML) algorithms found that Gaussian processes (GP) are a reliable alternative to model impacts and vulnerability (Côté et al., 2024). The present article improves the GP modelling by introducing more precise air pollution estimates and vegetation features.

2. Materials and methods

Unlike distributed lag non-linear models (DLNM) that require selecting temperature percentiles for spline knots (Gasparrini & Leone, 2014) or Poisson regressions using propensity score matching that requires a precise definition of heat waves (Kanti et al., 2022), AI and ML algorithms do not rely on specific definitions. The temperature-mortality relationship is established during the training process and validated during testing. In this article, figures using temperature thresholds (28, 30 and 32 °C) are only shown to provide a better understanding of the data to the reader. These thresholds are not coded in the GP model.

Epidemiological studies with appropriate cohorts to adjust for confounding variables remain the gold standard for assessing the relationship between exposure and outcomes (Djulbegovic & Guyatt, 2017; Kwakkenbos et al., 2021). Nevertheless, they are not the best option to perform a comprehensive risk assessment on a large territory without the possibility of forming cohorts. The first step to select features for the GP model is to identify their association with mortality during heat waves. Due to the *curse of dimensionality* and the necessity of maintaining a simple risk model (Chen et al., 2020), several features have been rejected due to their limited contribution to improving algorithmic performance. All features that are presented in this section have been tested in various models. The reader should not interpret the exclusion of a variable in the results section as an absence of association or relevance to adaptation to heat waves. Rather, it serves as a limit of the modelling process. This issue will be further discussed in the Discussion.

The projections for this study are made for the 2031, 2051, 2071, and 2091 censuses that each cover 5 years. Values between those years that are shown in the figures throughout this article are interpolated. This was done to reduce the amount of computation and is sufficient to provide reliable projections that guide decision making. The goal of the projections is not to accurately predict the mortality for a given year, but to provide an order of magnitude variation that could accommodate future scenarios.

2.1. Region description

A map of the City of Montreal is available in Section 3.2 (Fig. 7). To maintain case study conciseness, we focus on this region, but there are no technical limitations to extending the analysis to other regions. Processing Landsat images to extract the normalized difference vegetation index (NDVI) within a 300 m radius around each address centroid over a large territory, such as the Province of Quebec or Canada, and collecting daily air pollution data with good spatial resolution, are the two most involved steps in the pipeline to extend this methodology, but this is feasible with sufficient time and resources.

2.1.1. Temperatures

High temperatures are associated with higher mortality, but the precise definition of a heat wave remains an open question and depends on the study region (Conti, et al., 2022). Many definitions exist that are based on the duration, intensity, and inclusion of various temperature indicators, such as the minimum temperature at night, the mean daily temperature, and the maximum daily temperature (Guo et al., 2017; Xu et al., 2018). Even if we do not need to select a temperature threshold that is based on percentile or absolute values for GP to work, we tested various lags (1 to 7 days) and temperature indicators (minimum, mean, and maximum temperature) based on these definitions to optimize the results.

Fig. 1 compares the temperature trend between the historical data and various climate projections. Fig. 1(a) includes historical values from Daymet dataset providing a 1 km × 1 km grid for various variables, such as daily temperature for North America (Thornton et al., 2021). Gridded climate datasets provide similar results to ground stations and are suitable for epidemiological studies to provide temperature between weather stations that are not distributed homogeneously in the area of interest (Ahn et al., 2024; de Schrijver et al., 2021; Spangler et al., 2019; Thomas et al., 2021). Daymet only provides the value for the mean daily vapour pressure, which is not usable in calculating the relative humidity for the daily maximum temperature. We tested the mean daily humidity levels to predict the daily mortality, without success, but did not investigate further, given that more research is needed to clarify the role of humidity on mortality (Baldwin et al., 2023; Lo, et al., 2023; Simpson et al., 2023). Another limitation of Daymet is the absence of wind speed. Therefore we cannot use a heat metric like the Universal Thermal Climate Index (UTCI). Yet, because no heat metric has shown a clear superiority for epidemiological study (Rachid & Qureshi, 2023; Spangler et al., 2023) and some studies showed that the UTCI might not capture the indoor thermal stress well (Katal et al., 2023; Rajagopalan et al., 2020), this is not a limitation for our study.

The ClimateData.ca portal has been used to extract projection values with bias correction from 26 different Global Climate Models (GCMs) in the Coupled Model Intercomparison Project 6 (CMIP6) that have been downscaled to a 6 × 10 km grid for Canada (Cannon et al., 2015; ClimateData.ca, 2024; McKenney et al., 2011). Figs. 1(b), 1(c), and

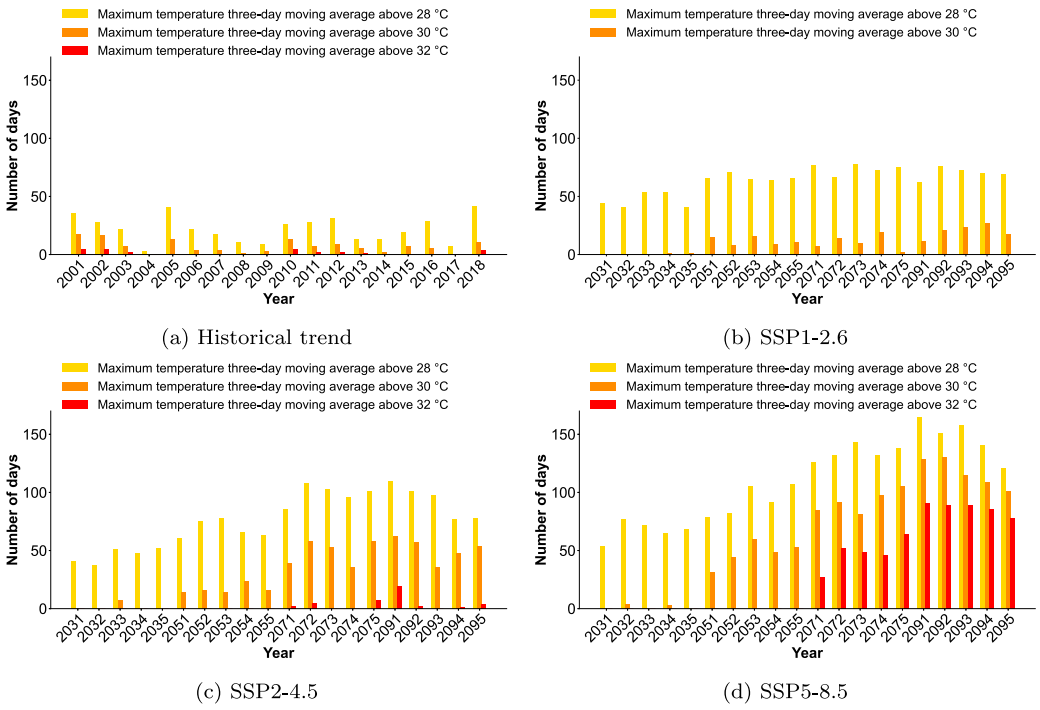

Fig. 1. Yearly number of hot days (based upon three increasing temperature thresholds) between 2001 and 2018 and for the median scenario of each SSP for the 2031, 2051, 2071 and 2091 census periods. (For interpretation of the references to colour in this figure legend, the reader is referred to the web version of this article.)

1(d) show how the intensity of heat waves will increase as the climate warms up. The median scenario for the optimistic projection in Fig. 1(b) does not have heat waves over 32 °C, whereas the median scenario for the pessimistic scenario in Fig. 1(d) has close to 100 days of intense heat waves. Projections are not predictions; they are only descriptions of what could happen if human societies make various decisions. O'Neill, et al. (2017) provide a brief description of different scenarios. SSP1-2.6 is usually associated with a future in which sustainable development decisions are made to reach the Paris Agreement. Although countries are far from being on track for this projection (den Elzen et al., 2022; Jewell & Cherp, 2020; Stoddard et al., 2021), it can be usefully employed as a baseline to remind the public and policymakers of the cost of inaction. SSP2-4.5 refers to the business-as-usual (BAU) scenario in which countries are aware of the problem but are unable to act decisively to solve it. SSP5-8.5 is the worst-case scenario that could occur if we burn most of the known planetary fossil fuel reserves. Even if this scenario is unlikely, it would not be impossible if we were not careful (Kemp et al., 2022) or if increasing geopolitical tensions were to drive society away from a BAU scenario (Ding et al., 2023; Zakeri, et al., 2022). Therefore, this is standard practice in the scientific literature to analyse the interval between the most optimistic scenario (SSP1-2.6) and the worst scenario (SSP5-8.5) to cover the range of possibilities (Chow et al., 2024; Sobie et al., 2024).

2.1.2. Mortality rate

Mortality data between 2001 and 2018 originates from the Registre des évènements démographiques - Fichier des décès (Ministère de la Santé et des Services sociaux (MSSSS), 2023) and are geolocalized with the Postal Code Conversion File + (PCCF+) (Statistics Canada, 2018). The complete data set was used and no sampling was performed.

Fig. 2 shows the increase in the mean daily mortality rate for daily maximum temperature with a three-day moving average above 28 °C for the historical period for the region. The higher mortality rate at the beginning of the study period is explained in part by lower life expectancy (see the Age section) and less favourable life conditions (see the Socioeconomic variables and air pollution section).

Interannual variability helps in understanding how differences between the years in the training and testing datasets can yield varying results. If every year with intense heat waves is included in the testing dataset, the algorithm would not be able to detect the trend in the training process and will perform poorly. Conversely, if all intense heat waves are in the training dataset, the root-mean-square error (RMSE) might be very good for most predictions in the testing dataset with normal temperatures, yet this would not necessarily indicate effective pattern detection during heat waves.

Life expectancy is not included as a feature, given that its addition would result in data leakage. In other words, introducing an input feature (life expectancy) that is derived from the target (the mortality rate) could allow the algorithm to detect this pattern, rendering it ineffective for making generalizable predictions.

These details are often overlooked in studies using AI and ML, yielding excellent results on paper but poor results in real settings (Buczynski et al., 2021; Kelly et al., 2019). To avoid this pitfall, we provide more information regarding the manner in which we split the training and test datasets into multiple models in the Features summary section.

2.1.3. Age

Fig. 3(a) shows the historical trend in the proportion of older population for the Montreal region. Data are from Statistics Canada (2001, 2006, 2011, 2016b, 2021) censuses and values between censuses were linearly interpolated. The proportion of people over the age of 75 is increasing during the study period and is closely correlated with the increase in life expectancy that averaged 79.5 in 2001 and 83.1 in 2018 (Institut de la statistique du Québec, 2024).

Despite SSP scenarios providing a narrative for aging, we include three different scenarios regardless of the temperature pathway. SSPs are for global trends and do not make projections for a specific country. We used three different projections from Statistics Canada in which migration levels, birth rates, and mortality rates lead to different demographic trends (Statistics Canada, 2022). Fig. 3(b) shows a scenario in which the population above 65-years-old will stabilize and decrease slightly around 2050, Fig. 3(c) shows an intermediate scenario in which the historical trend of aging is maintained, and Fig. 3(d) shows a

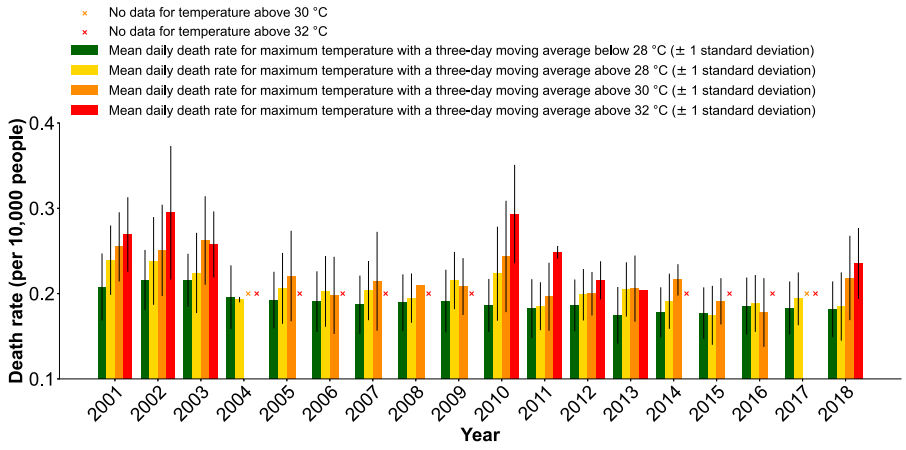

Fig. 2. Mean daily death rate between 2001 and 2018 for maximum temperatures with three-day moving average thresholds below 28 °C , and above 28 °C , 30 °C and 32 °C. (For interpretation of the references to colour in this figure legend, the reader is referred to the web version of this article.)

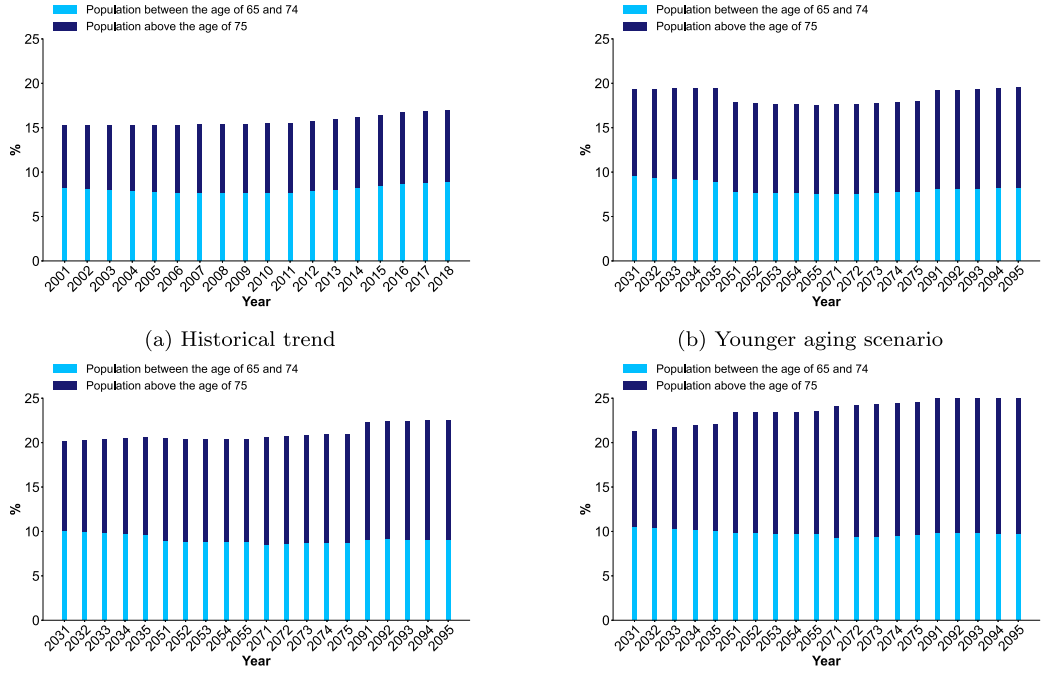

Fig. 3. Yearly percentage of older population for the historical period and projections for the 2031, 2051, 2071 and 2091 census periods based on data from Statistics Canada. (For interpretation of the references to colour in this figure legend, the reader is referred to the web version of this article.)

scenario in which aging accelerates and leads to a high proportion of people over 65 years of age.

2.1.4. Socioeconomic variables and air pollution

Meta-analyses have concluded that short- and long-term exposure to $PM_{2.5}$, NO_2, and O_3 is detrimental to human health (Dominski, et al., 2021; Li et al., 2017; Orellano et al., 2020; Yang et al., 2019). Fig. 4(a) shows the historical trend for the mean annual pollutant concentrations from the ground stations in the city. We used daily concentration in our models; this figure is only to give an insight of the general trend to the reader. Unfortunately, these air-quality monitoring stations changed locations across the study period, are not uniformly distributed, and are not in sufficient numbers to use sophisticated interpolation techniques like kriging. Therefore, we use simple inverse distance weighting (IDW) between stations to create a raster with a 1 km × 1 km that covers the entire region of interest.

Fig. 4(b) shows the improvement in socioeconomic variables over time regarding the population without a degree and the population below the low income cut-offs (LICO) as defined by Statistics Canada (2016a). The improvement of these metrics corresponds to an improvement in life expectancy (see Section 2.1.3). Having a neighbourhood with an unfavourable profile for these metrics is associated with a higher mortality rate during heat waves (Arsad et al., 2022).

2.1.5. Vegetation

Vegetation is associated with a decrease in heat-related mortality in urban environments (Choi, et al., 2022; Dardir et al., 2023; Rojas-Rueda et al., 2019; Sinha et al., 2022); hence, its inclusion in the model. Vegetation cover has been estimated with an NDVI that was calculated from Landsat 5, 7 and 8 image collections with a resolution of 30 m × 30 m (Young et al., 2017). Given that a Landsat satellite acquires an image every 16 days for a specific location, combining two different missions can help to increase the number of exploitable

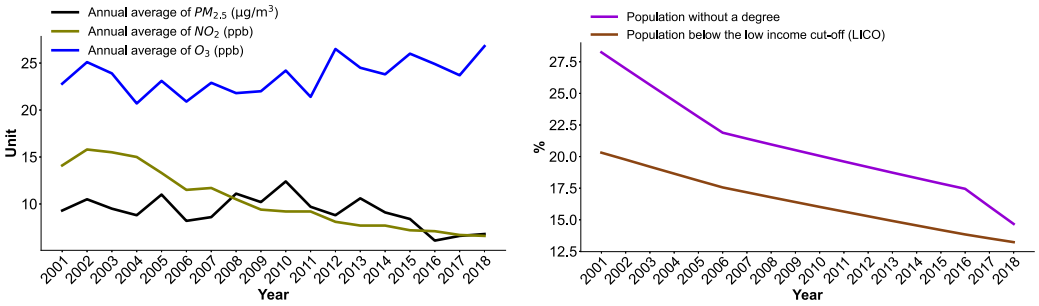

(a) Yearly average concentration of $PM_{2.5}$ ($\mu g/m^3$), NO_2 (ppb) and O_3 (ppb) between 2001 and 2018

(b) Yearly percentage of population below the low income cut-off or without a degree

Fig. 4. Historical trends for air pollution and socioeconomic variables. (For interpretation of the references to colour in this figure legend, the reader is referred to the web version of this article.)

images without clouds during the narrow window when vegetation is at maturity. To reduce sensor noise between generations and the effects of summers with less exploitable images where vegetation reaches its peak greenness, a Savitzky-Golay filter has been used (Chen et al., 2004). This filter helps to smooth out the yearly trends throughout the study period. Small annual variation can be explained in part by freezing rain that can kill mature trees (Armenakis & Nirupama, 2014) and by the epidemic of *Agrilus planipennis*, i.e., the emerald ash borer (Wood & Dupras, 2021), which can lead to the replacement of mature trees. Despite the precautions and filters that are used, cloudy summers that decreased the number of exploitable Landsat images during leaf-out and blossoming can also explain these slight variations.

Based on our data and the literature, every pixel with an NDVI value greater than 0.3 was considered vegetation that was suitable for reducing the urban heat island effect (UHI) (Heinl et al., 2015; Weng et al., 2004). To model exposure to vegetation as accurately as possible, the centroid of each residential address was used to calculate the number of surrounding pixels with the presence of suitable vegetation. The addresses come from Adresses Québec (AQ) (Ministère des ressources naturelles et des forêts, 2024), which also include the number of units that can be translated into the number of households.

The percentage of pixels with adequate vegetation surrounding a household was calculated based on different radii. There is no consensus in the literature regarding the optimal radius that should be considered around a household for mortality and health outcomes, but typically it varies between 100 m and 1 km (Liu et al., 2022; Rojas-Rueda et al., 2019). Figs. 5(a) and 5(b) respectively show the percentage of households with at least 30% and 50% vegetation within a radius of 100 m and 300 m. The trend is similar regardless of the radius size, but a higher proportion of households reach the threshold 30% with a radius of 300 m.

A key variable that should be integrated into the analysis is the average size of a household. Fig. 5(c) shows the correlation between household size and the percentage of households in an aggregate dissemination area (ADA) (Statistics Canada, 2016a) with at least 30% vegetation within a radius of 300 m. Without this adjustment to the model, the percentage of the population that is surrounded by suitable vegetation is underestimated, which yields unstable results.

The general increasing trend for vegetation can be explained by the decrease in the construction of new buildings, neighbourhood densification, and the increase in the number of households per address (see Fig. 5(d)). Yet, future trends are difficult to extrapolate from these historical data. The Canadian housing shortage crisis, together with the inflation that cripples government budgets, thereby leading to a lack of political will to change the taxation system that is directly related to property values (Farhan, 2024), are examples of immediate problems that can overshadow long-term goals of protecting ecosystems (Picketts, 2018). Other barriers such as a general lack of political leadership, a lack of public awareness that would push for political changes, and the misalignment of policies between local, provincial, and federal governments (Oulahen et al., 2018) illustrate how increasing vegetation in urban areas is not trivial despite its obvious mitigation potential and health benefits (Sharifi et al., 2021).

2.1.6. Features summary for each model

The choice of training and testing datasets can negatively affect the generalization of the algorithm. Therefore, to avoid potential bias in the projections, we used five models that have five different training and test datasets. Each year is selected only once to be included in a testing set, and the years within each set have a 5-year interval gap. This way of splitting the data has the advantage of guaranteeing a few heat waves in each model. Such would not be the case if we were to perform random cross-validations. Furthermore, selecting the data with simple predetermined rules ensures that the models are robust and are not the result of experimenter "cherrypicking" of the data to increase performance artificially. The summary of each model is provided in Table 1.

The models are well balanced for socioeconomic features, as expected, since every census is represented once, but some exhibit variability in temperature. The implications of this variability for mortality rate projections will be discussed in the Historical impacts results section.

2.2. Gaussian processes and SHAP values

A Gaussian process (GP) is a well-known non-parametric algorithm with a wide variety of uses. Its time complexity of $\mathcal{O}(n^3)$ limited its use in the past, but recent developments in graphics processing units (GPU) and algorithms have alleviated this inconvenience in recent years (Liu et al., 2020). For the theoretical foundation, the reader can refer to Rasmussen and Williams (2006). In summary, a GP can be defined as

$$f(x) \sim GP(m(x), k(x, x'))$$

where m is the mean function that is usually set to zero and k is the covariance function, which is also known as the kernel. Some commonly used kernels are linear, polynomial, squared exponential (also known as a radial basis function) and kernels from the Matérn family (1/2, 3/2, 5/2). Kernels can be added or multiplied together over different dimensions of the input. Each kernel has parameters to fit the equation to the data. Machine-learning algorithms can automatically find these parameters to obtain the best fit, but the search for the optimal kernel composition is based on the knowledge of the modeller, together with some trial-and-error. For example, you can use the following equation for the squared exponential kernel

$$k(x_i, x_j) = \sigma^2 \exp\left(-\frac{(x_i - x_j)^2}{2\ell^2}\right)$$

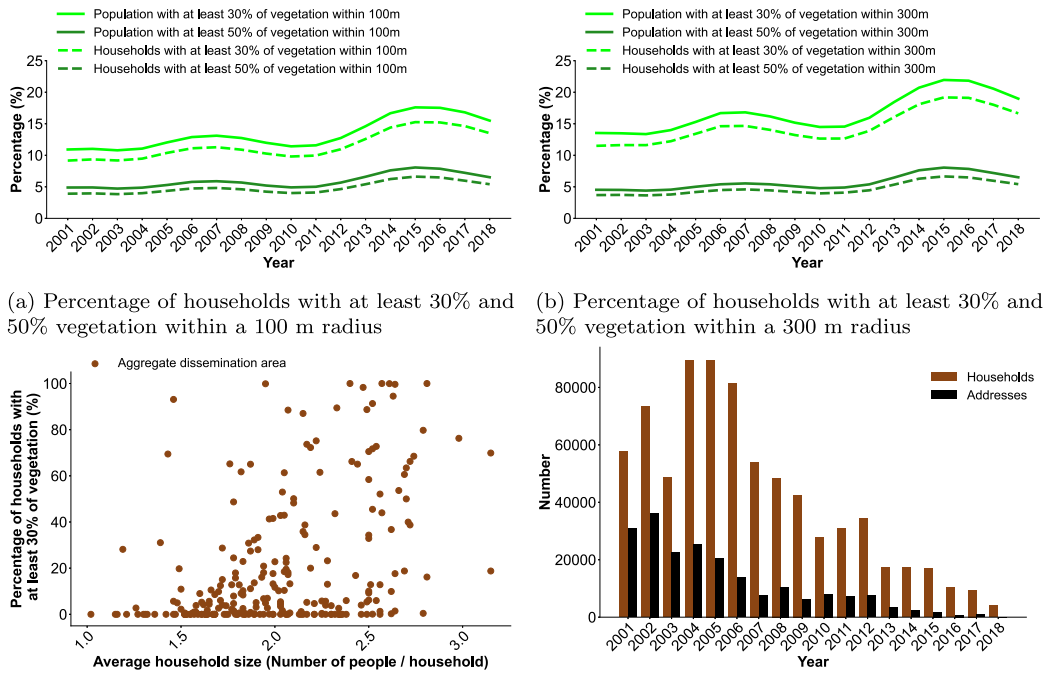

(a) Percentage of households with at least 30% and 50% vegetation within a 100 m radius

(b) Percentage of households with at least 30% and 50% vegetation within a 300 m radius

(c) Average household size and percentage of households with at least 30% vegetation within 300 m

(d) Yearly new addresses and households

Fig. 5. Historical vegetation level trends. (For interpretation of the references to colour in this figure legend, the reader is referred to the web version of this article.)

Table 1
Overview of socioeconomic, temperature, air pollution and vegetation features based on the test years.

Features	Model 1	Model 2	Model 3	Model 4	Model 5
Test years	2001	2002	2003	2004	2005
	2006	2007	2008	2009	2010
	2011	2012	2013	2014	2015
	2016	2017	2018		
Population above age 65 (%)	15.7	15.81	15.92	15.65	15.75
Population between age 65 and 74 (%)	8.06	8.11	8.16	7.95	7.98
Population between age 75 and 84 (%)	5.48	5.49	5.5	5.53	5.54
Population above age 85 (%)	2.16	2.21	2.26	2.17	2.23
Population without a degree (%)	16.84	16.43	16.03	16.53	16.1
Low income cut-offs after tax (LICO) (%)	21.8	20.9	20.01	21.07	20.36
Renter (%)	59.24	59.12	58.99	59.04	58.84
One-person household (%)	17.22	17.3	17.38	17.26	17.32
Mean maximum temperature three-day moving averages (°C)	24.58	24.39	24.25	23.26	24.77
Number of observations where the maximum temperature three-day moving averages ≥ 28 °C	115	84	88	26	86
Number of observations where the maximum temperature three-day moving averages ≥ 30 °C	37	30	25	5	33
Number of observations where the maximum temperature three-day moving averages ≥ 32 °C	7	7	7	0	5
Mean NO_2 (ppb) three-day moving averages	10.46	10.57	10.09	10.69	9.92
Minimum 30% vegetation within 300 m (%)	16.65	16.7	16.74	16.63	17.24

where σ^2 is the overall variance and ℓ is the length-scale parameter learned in the training process.

For a more in-depth explanation of GP, the readers can refer to Roberts et al. (2013), Schulz et al. (2018), and Wang (2023) for practical guidance on how to use GP for modelling, to Duvenaud (2014) for help in choosing kernels, and to Marrel and Iooss (2024) for a review of kernel parameters.

SHapley Additive exPlanations (SHAP) can help increase the interpretability of the model by providing a measure of the importance of features (Lundberg & Lee, 2017). This technique for explainable AI (XAI) is based on game theory to evaluate the contribution of each feature to the prediction. A SHAP value neither implies causation nor does it have a value that is easy to interpret outside of the model context. Yet, inclusion of SHAP values alleviates the black-box effect of AI and ML models and is widely used by practitioners and researchers (Ali et al., 2023; Allgaier et al., 2023; Loh et al., 2022; Vimbi et al., 2024).

2.3. Software

Data processing and visualization were performed in Python (Van Rossum & Drake, 2009) with the standard scientific libraries Numpy (Harris et al., 2020), Pandas (McKinney, 2010), Xarray (Harris et al., 2020), and Matplotlib (Hunter, 2007). Maps have been produced with QGIS (QGIS Development Team, 2024). GP has been performed with GPFlow (Matthews, et al., 2016) and SHAP values originate from the python SHAP library (Lundberg & Lee, 2017). Google Earth Engine (GEE) Python API has been used to extract Daymet and Landsat images (Gorelick et al., 2017).

Table 2
Features and kernels for the daily mortality rate.

Features	Kernels
Maximum temperature three-day moving averages	Matern 5/2
Population above the age 65	Linear
Low income cut-offs after tax (LICO)	Linear
Daily mean NO_2 (ppb) three-day moving averages	Matern 5/2
Minimum 30% vegetation within 300 m	Matern 3/2
Week	Squared exponential

Table 3
Historical results for the daily mortality rate per 10,000 people.

Maximum temperature three-day moving averages (°C)	Statistics	Model 1	Model 2	Model 3	Model 4	Model 5
	RMSE	0.036	0.033	0.033	0.034	0.032
	Actual annual mean	0.191	0.193	0.190	0.189	0.185
< 28	Predicted annual mean	0.193	0.189	0.189	0.190	0.187
	(95% CI)	(0.191, 0.194)	(0.188, 0.191)	(0.188, 0.190)	(0.188, 0.191)	(0.186, 0.188)
	Actual daily max	0.309	0.330	0.301	0.322	0.272
	Predicted daily max	0.228	0.226	0.225	0.219	0.221
	(95% CI)	(0.163, 0.293)	(0.158, 0.293)	(0.157, 0.293)	(0.154, 0.284)	(0.153, 0.288)
	RMSE	0.035	0.036	0.035	0.033	0.041
	Actual annual mean	0.206	0.213	0.199	0.197	0.204
≥ 28	Predicted annual mean	0.209	0.208	0.204	0.193	0.208
	(95% CI)	(0.204, 0.213)	(0.204, 0.213)	(0.200, 0.209)	(0.190, 0.197)	(0.204, 0.211)
	Actual daily max	0.326	0.391	0.318	0.272	0.383
	Predicted daily max	0.305	0.276	0.273	0.209	0.252
	(95% CI)	(0.235, 0.376)	(0.208, 0.344)	(0.202, 0.344)	(0.144, 0.274)	(0.184, 0.320)
	RMSE	0.038	0.041	0.045	0.023	0.049
	Actual annual mean	0.222	0.231	0.227	0.211	0.223
≥ 30	Predicted annual mean	0.231	0.230	0.226	0.201	0.219
	(95% CI)	(0.221, 0.24)	(0.222, 0.238)	(0.216, 0.236)	(0.197, 0.205)	(0.214, 0.224)
	Actual daily max	0.326	0.391	0.318	0.235	0.383
	Predicted daily max	0.305	0.276	0.273	0.205	0.252
	(95% CI)	(0.235, 0.376)	(0.208, 0.344)	(0.202, 0.344)	(0.140, 0.270)	(0.184, 0.320)
	RMSE	0.036	0.059	0.041		0.072
	Actual annual mean	0.263	0.272	0.237		0.293
≥ 32	Predicted annual mean	0.277	0.258	0.259	N/A	0.240
	(95% CI)	(0.259, 0.295)	(0.241, 0.275)	(0.247, 0.27)		(0.228, 0.252)
	Actual daily max	0.326	0.391	0.285		0.383
	Predicted daily max	0.305	0.276	0.273		0.252
	(95% CI)	(0.235, 0.376)	(0.208, 0.344)	(0.202, 0.344)		(0.184, 0.32)

3. Results

3.1. Historical impacts for the daily mortality rate

Table 2 shows the features and their associated kernel that were added to achieve the best performance across different temperature thresholds. Studies using AI and ML to predict mortality for Montreal have found similar results for the lag period and the importance of NO_2 in the predictions (Boudreault et al., 2023, 2024a).

Table 3 includes the RMSE for each model and temperature threshold. The results for temperatures below 28 °C are consistent across models. Model performances diverge for temperatures above 32 °C. As explained in the Features summary section, model 5 has the most intense heat waves in the test dataset. Therefore, the training model cannot detect the trend and fails to make accurate predictions where actual values are not even comprised within the prediction 95% confidence interval. Model 2 also experiences difficulty in predicting peak mortality for the test dataset, but can predict the mean annual daily mortality rate within its 95% confidence interval.

Fig. 6 provides the daily mortality rate for 2010 and 2018. These two years correspond to the most recent and intense heat waves that struck the region. The low mortality rate that was observed at the end of heat waves in both figures could be due to mortality displacement (harvesting effect), where peak mortality is followed by a lower mortality rate, since most frail individuals have already died during the initial shock (Cheng et al., 2018). This response could partially explain why models have a tendency to underestimate peak mortality during intense heat waves. By averaging out the peak mortality and the aforementioned mortality displacement, GP does not model each phenomenon accurately, yet still provides a good general trend during heat waves, except for the most intense ones. Figs. 6(c) and 6(d) show the SHAP values for the model making the predictions. SHAP values yield the expected trends describe in Section 2. High temperature, old age and a low income all contributes to increase mortality. The small yearly improvement in air quality and vegetation level over the region contribute marginally to the prediction.

3.2. Historical vulnerability for the summer mortality rate across ADA

The purpose of the vulnerability assessment is to understand how the mortality rate differs among neighbourhoods. Due to the daily increase of 0.05 deaths per 10,000 people during a heat wave, finding good temporal and spatial resolution is challenging. The smallest geographical unit that obtained significant results was the aggregate dissemination area (ADA, i.e., a geographic area delimited for collecting census data), which on average contain between 5,000 and 15,000 people (Statistics Canada, 2016a). The best temporal resolution was for the entire period between May and September. We removed any ADAs that contained fewer than 1000 people to maintain statistical power. A total of 251 ADAs in our study region met this criterion.

Table 4 shows the features and their associated kernels that were added to achieve the best performance in predicting whether each ADA has a summer mortality rate near or far from the region average.

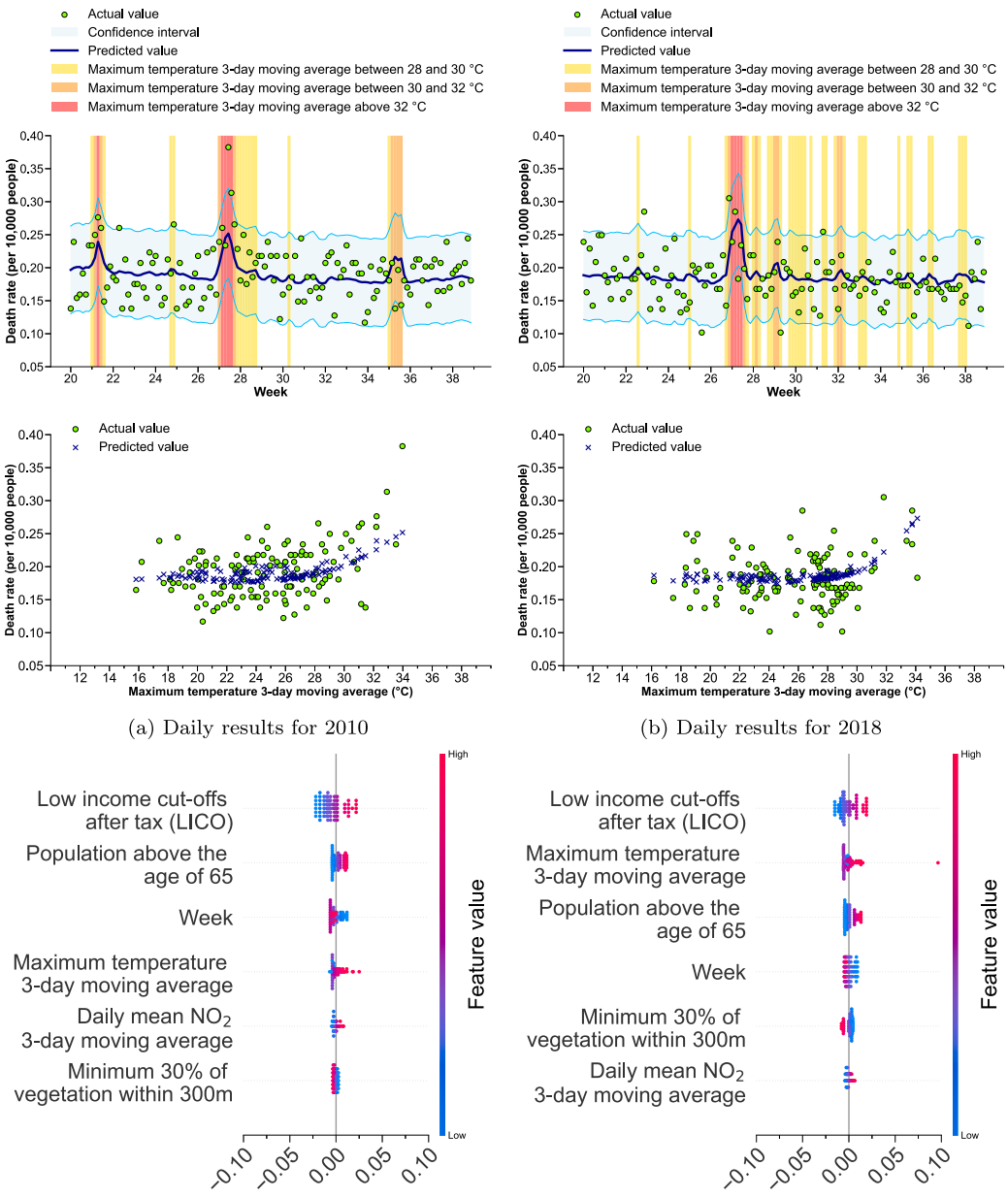

(a) Daily results for 2010

(b) Daily results for 2018

(c) SHAP values for model 5 for daily results

(d) SHAP values for model 3 for daily results

Fig. 6. Results for the historical mortality daily rate. (For interpretation of the references to colour in this figure legend, the reader is referred to the web version of this article.)

Table 4
Features and kernels for summer mortality rates across neighbourhoods.

Features	Kernels
Population above age 85	Squared exponential
Population between age 75 and 84	
Population between age 65 and 74	
One-person household	
Population without a degree	
Low income cut-offs after tax (LICO)	
Renter	
Minimum 30% vegetation within 300 m	

As explained in the Introduction, vulnerability encapsulates sensitivity and adaptive capacity. The algorithm does not distinguish between sensitivity and adaptive capacity, but it can be useful in making a distinction at a conceptual level to aid in decision making. Based on Côté et al. (2024), variables that cannot be changed within the scope of an adaptation plan, such as age and socioeconomic variables, should be considered as sensitivity. Adaptive capacity would include every variable that can be modified with adaptation strategies within an adaptation plan.

Air pollution would have been an interesting variable to incorporate into the vulnerability model. Unfortunately, as mentioned in Socioeconomic variables and air pollution section, the low density of air-quality monitoring stations could not provide appropriate spatial resolution to discriminate between ADAs. The percentage of the population with at least 30% vegetation within 300 m is the only feature that we could use effectively, and which fits the definition of adaptive capacity.

Figs. 7(a) and 7(b) show the map for the actual and predicted vulnerability for 2018. The further an observation departs from the summer mean mortality rate for the region, the more or less vulnerable the ADA is considered. Some variables in the SHAP values in Fig. 7(c)

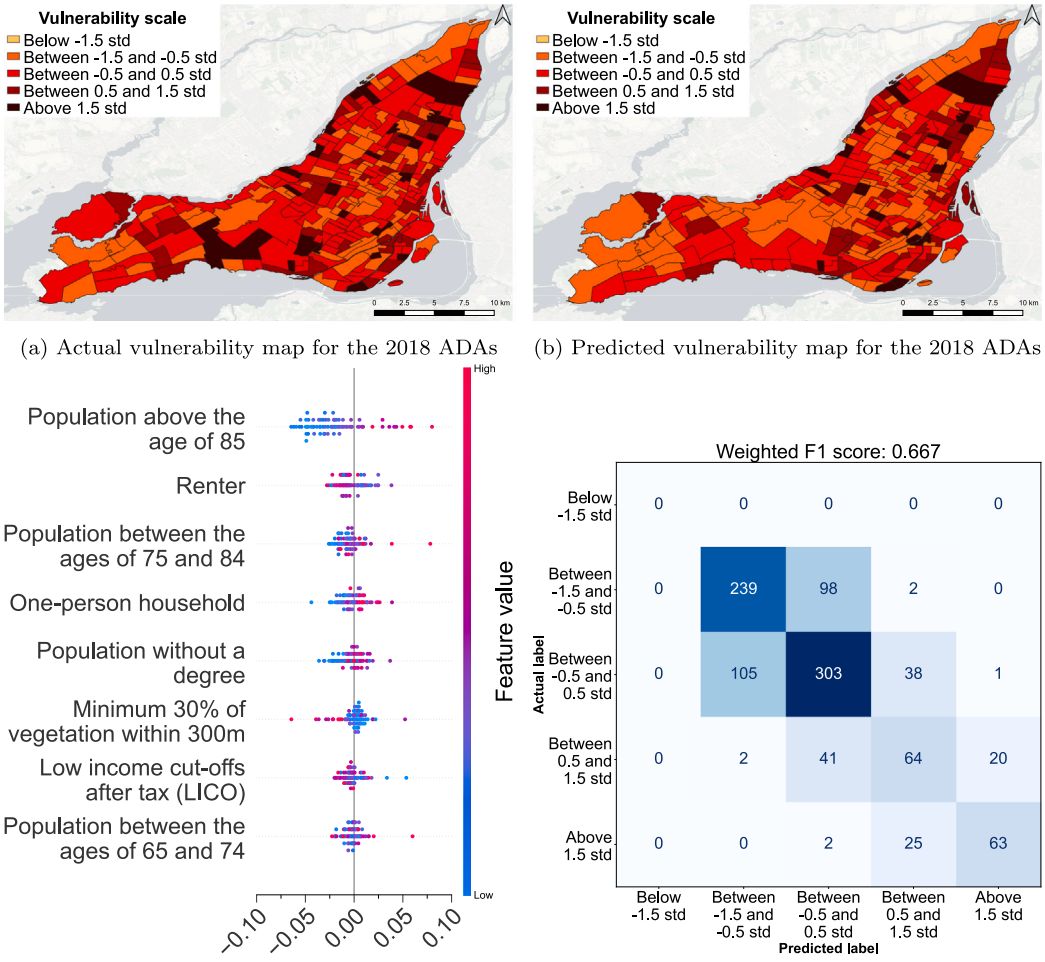

(a) Actual vulnerability map for the 2018 ADAs

(b) Predicted vulnerability map for the 2018 ADAs

(c) SHAP values for the predicted map

(d) Confusion matrix for the model that is used to predict the map

Fig. 7. Results for historical vulnerability. (For interpretation of the references to colour in this figure legend, the reader is referred to the web version of this article.)

might be surprising and contradict common social vulnerability indexes (Mah et al., 2023). For instance, being a renter and having a low income does not necessarily translate into higher mortality. This trend makes sense if we consider that the large student community in Montreal is more likely to be renters and below the LICO, but not at a higher risk of mortality. Yet, removing any of these variables decreased the weighted F1 score (the harmonic mean of precision and recall) by a few percent. Taken separately, each feature does not predict the mortality rate well, but their combination when added to old age is an adequate predictor. Vegetation plays a much bigger role in the vulnerability assessment, because the difference between neighbourhoods can be as high as 70%, which is more significant than a difference of a few % between each model in the impact assessment. The confusion matrix in Fig. 7(d) shows that the algorithm is usually just one category off. Therefore, despite having only an average F1 score for every model in Table 5, we still achieve a reasonable estimate in locating the most vulnerable neighbourhood, where efforts for climate adaptation should be focused. The confusion matrix reveals a category imbalance, so an overall accuracy metric would not be useful. It also shows that SVIs that usually use quintile to classify vulnerability are probably wrong, since vulnerability is not normally distributed.

In the absence of credible projections for each ADA, we projected the 2018 vulnerability trend to future scenarios. As explained in the Vegetation section, a case could be made for either pessimistic or optimistic scenarios, as well as for the status quo. Therefore, to keep the article as simple as possible by limiting the number of hypothetical scenarios, we only modified the age and temperature at the regional level to assess the projected regional daily mortality rate in the next section.

Table 5
Weighted F1 score for every model.

	Model 1	Model 2	Model 3	Model 4	Model 5
Weighted F1 score	0.649	**0.667**	**0.667**	0.654	0.631

3.3. Projected impacts for the daily mortality rate

Despite some discrepancies between models as described in Section 3.1, the general trends are preserved and conclusions can be drawn from the projection of the summary plot for each model in Fig. 8(d).

As expected, age contributed to a substantial increase in mortality (Figs. 8(a), 8(b), and 8(c)). The larger projection range for the older aging scenario can be explained by the fact that we have to extrapolate more for this scenario because it departs more strongly from historical values than the younger scenario (see age section). Temperature becomes a bigger factor after 2050, when the SSPs begin to diverge.

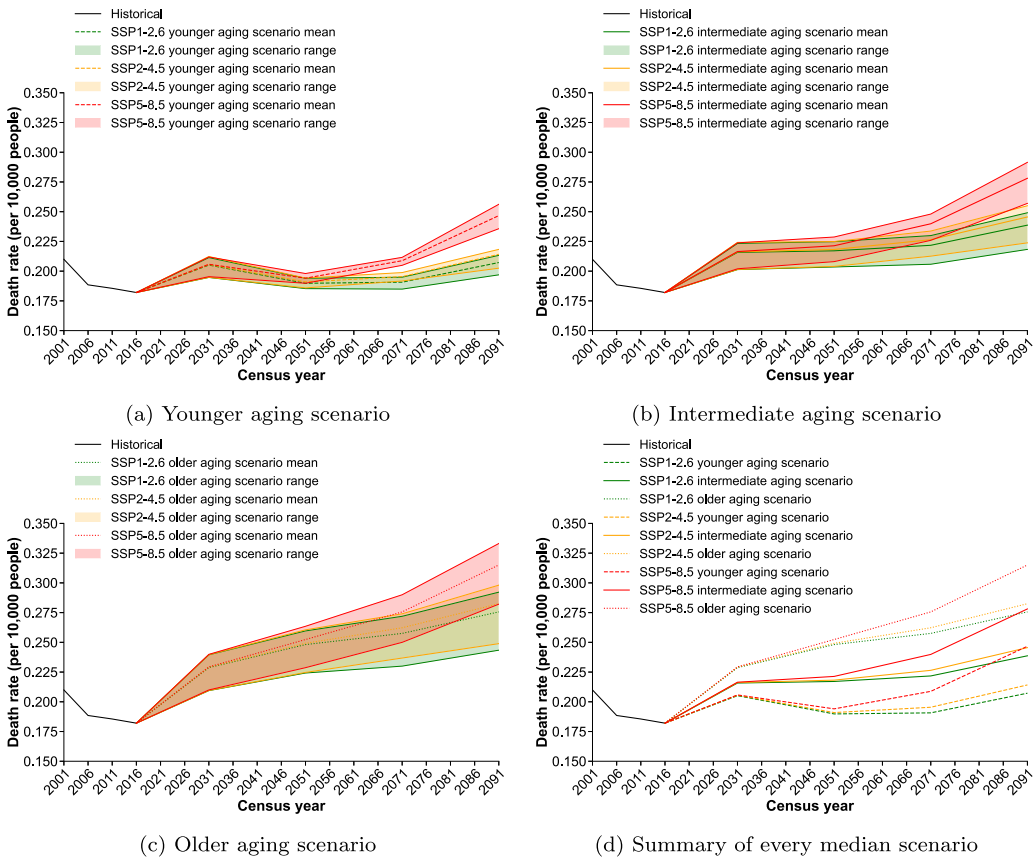

Fig. 8. Results for the yearly projected mean daily mortality rate. (For interpretation of the references to colour in this figure legend, the reader is referred to the web version of this article.)

Table 6
Projected mean annual mortality rate per 10,000 people for the median scenario (95% CI).

Aging scenarios	SSP scenarios	2031	2051	2071	2091
Younger	SSP1-2.6	0.205 (0.205, 0.206)	0.190 (0.189, 0.190)	0.191 (0.190, 0.191)	0.207 (0.207, 0.208)
	SSP2-4.5	0.206 (0.205, 0.206)	0.191 (0.190, 0.191)	0.195 (0.195, 0.196)	0.214 (0.213, 0.215)
	SSP5-8.5	0.206 (0.205, 0.206)	0.194 (0.193, 0.195)	0.209 (0.207, 0.210)	0.247 (0.244, 0.249)
Intermediate	SSP1-2.6	0.216 (0.215, 0.216)	0.217 (0.216, 0.218)	0.222 (0.221, 0.222)	0.239 (0.238, 0.240)
	SSP2-4.5	0.216 (0.216, 0.217)	0.218 (0.217, 0.219)	0.226 (0.226, 0.227)	0.246 (0.244, 0.247)
	SSP5-8.5	0.216 (0.216, 0.217)	0.221 (0.220, 0.222)	0.240 (0.238, 0.241)	0.278 (0.276, 0.281)
Older	SSP1-2.6	0.229 (0.228, 0.230)	0.248 (0.247, 0.249)	0.258 (0.256, 0.259)	0.276 (0.274, 0.277)
	SSP2-4.5	0.229 (0.228, 0.230)	0.249 (0.248, 0.250)	0.262 (0.261, 0.264)	0.283 (0.281, 0.284)
	SSP5-8.5	0.229 (0.228, 0.230)	0.252 (0.251, 0.254)	0.276 (0.274, 0.277)	0.315 (0.312, 0.318)

Tables 6 and 7 show the values from the median projected scenario. Tables 8 and 9 show the percentage change when compared to SSP1-2.6. These results are consistent with other studies for the Montreal region (Doyon et al., 2008; Hebbern et al., 2023; Martin et al., 2012).

If the increase in the mean annual daily mortality rate appears to align with historical values, the maximum daily mortality rate appears to be underestimated. The peak mortality in historical data reached 0.391 deaths per 10,000 people during heat waves. Yet, the model was unable to capture these peaks in the testing dataset; it shows up in the projection where only the most distant worse scenario (older population in SSP5-8.5) surpasses this threshold. This response is explored in greater detail in the Discussion.

4. Discussion

4.1. Limitations of this study

GP has been used to model mortality and make projections in various contexts with reliable results (Dhamodharavadhani & Rathipriya, 2021; Ludkovski et al., 2018; Monod et al., 2023; Wu & Wang, 2018). Yet, GP exhibits the same limitations as other well-known algorithms such as DLNM, namely the inability to accurately extrapolate beyond the boundaries of the observed historical data or to take into account complex future adaptation dynamics (Vicedo-Cabrera et al., 2019).

Table 7
Projected mean maximum daily mortality rate per 10,000 people for the median scenario (95% CI).

Aging scenarios	SSP scenarios	2031	2051	2071	2091
Younger	SSP1-2.6	0.224 (0.153, 0.294)	0.217 (0.152, 0.282)	0.211 (0.144, 0.279)	0.235 (0.167, 0.303)
	SSP2-4.5	0.224 (0.154, 0.295)	0.216 (0.151, 0.281)	0.230 (0.162, 0.297)	0.258 (0.191, 0.326)
	SSP5-8.5	0.225 (0.154, 0.295)	0.225 (0.160, 0.290)	0.273 (0.202, 0.343)	0.341 (0.256, 0.427)
Intermediate	SSP1-2.6	0.235 (0.162, 0.309)	0.246 (0.175, 0.317)	0.248 (0.177, 0.319)	0.272 (0.199, 0.345)
	SSP2-4.5	0.236 (0.163, 0.310)	0.245 (0.175, 0.316)	0.262 (0.192, 0.333)	0.293 (0.215, 0.372)
	SSP5-8.5	0.237 (0.163, 0.310)	0.256 (0.185, 0.326)	0.307 (0.232, 0.383)	0.377 (0.285, 0.469)
Older	SSP1-2.6	0.250 (0.174, 0.326)	0.279 (0.198, 0.360)	0.290 (0.212, 0.369)	0.315 (0.232, 0.398)
	SSP2-4.5	0.251 (0.172, 0.329)	0.278 (0.198, 0.359)	0.302 (0.215, 0.390)	0.335 (0.241, 0.429)
	SSP5-8.5	0.251 (0.175, 0.327)	0.292 (0.217, 0.368)	0.348 (0.258, 0.438)	0.418 (0.311, 0.526)

Table 8
Mean annual daily mortality rate percentage change compared to the SSP1-2.6 scenario from the same aging scenario (%).

Aging scenarios	SSP scenarios	2031	2051	2071	2091
Younger	SSP1-2.6	Baseline			
	SSP2-4.5	0.49	0.53	2.09	3.38
	SSP5-8.5	0.49	2.11	9.42	19.32
Intermediate	SSP1-2.6	Baseline			
	SSP2-4.5	0.00	0.46	1.80	2.93
	SSP5-8.5	0.00	1.84	8.11	16.32
Older	SSP1-2.6	Baseline			
	SSP2-4.5	0.00	0.40	1.55	2.54
	SSP5-8.5	0.00	1.61	6.98	14.13

Table 9
Mean maximum daily mortality rate percentage change compared to the SSP1-2.6 scenario from the same aging scenario (%).

Aging scenarios	SSP scenarios	2031	2051	2071	2091
Younger	SSP1-2.6	Baseline			
	SSP2-4.5	0.00	−0.46	9.00	9.79
	SSP5-8.5	0.45	3.69	29.38	45.11
Intermediate	SSP1-2.6	Baseline			
	SSP2-4.5	0.43	−0.41	5.65	7.72
	SSP5-8.5	0.85	4.07	23.79	38.60
Older	SSP1-2.6	Baseline			
	SSP2-4.5	0.40	−0.36	4.14	6.35
	SSP5-8.5	0.40	4.66	20.00	32.70

For example, there is some evidence that human physiology can adapt to a small increase in ambient temperature, leading to a decrease in mortality risk over time (Wu, et al., 2024). Yet, human thermoregulation and acclimatization are not infinite and represent a hard limit to the capacity to adapt (Hanna & Tait, 2015). The same can be said about the role of vegetation in decreasing human mortality. Even if vegetation is effective at decreasing mortality (Barboza, et al., 2021), it also has its limits (Gao et al., 2024; Pascal et al., 2021). Trees are also at risk of dying from heat waves and droughts, both within cities (Esperon-Rodriguez et al., 2022; Marchin et al., 2022) and well beyond urban environments (Hammond, et al., 2022). Therefore, their contributions to decreasing human mortality under pessimistic climate scenarios is uncertain.

With a better understanding of these phenomena, it would be possible to use this domain knowledge and incorporate it into GP models (Roberts et al., 2013). Unfortunately, to the best of our knowledge and based on a review by Cordiner et al. (2024), the optimal strategy for incorporating adaptation into models remains an open question in the literature.

As noted in the Results section, our models were unable to capture mortality peaks for the worst heat waves within the confidence intervals of the test datasets. Combining this fact with hard limits to adaptation, our pessimistic projections are probably vastly underestimating mortality, despite being in line with other studies for the region (Doyon et al., 2008; Hebbern et al., 2023; Martin et al., 2012). Optimistic projections might slightly overestimate mortality because we did not take into account possible future adaptation and acclimatization strategies. Therefore, it should be noted that projection uncertainty goes beyond the statistical confidence interval. Even when this uncertainty is taken into account, the models show that there will be negative consequences if we fail to adapt properly and mitigate GHG emissions.

Finally, by nature, modelling cannot incorporate all relevant variables within a single model, especially for adaptation to climate change, which is a broad topic with sparse local data. For example, $PM_{2.5}$ and O_3 are associated in the literature with an increase in mortality (Stafoggia et al., 2023). Their exclusion from our model does not imply their irrelevance, but rather imply the need for a better air-quality monitoring system that would allow us to improve the vulnerability assessment in a second model.

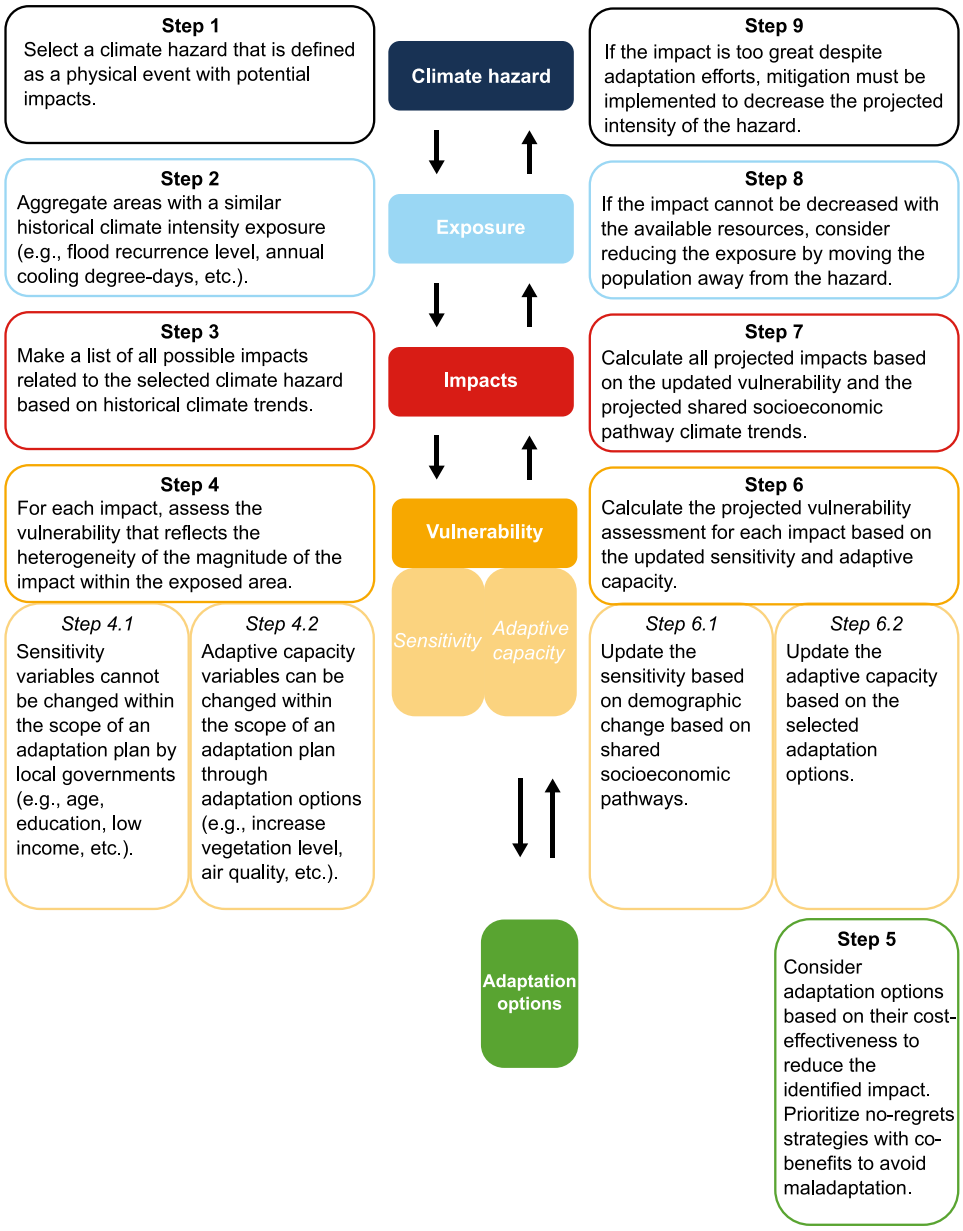

Fig. A.1. Flowchart to manage climate risk based on exposure, impacts and vulnerability.

To improve data collection for weather and air quality, an Internet of Things (IoT) network could be implemented (Park & Baek, 2023). Indoor temperatures could also be assessed via smart thermostats to better capture the thermal stress of dwellers (Oetomo et al., 2022). To improve vegetation exposure assessment, a combination of LiDAR and Landsat imagery could be interesting, even if NDVI appears to be reliable on its own (Ju et al., 2024). Yet, these examples underscore a constant trade-off between the availability of historical data and the improve precision of new technology, which can also be costly.

On a purely scientific level, we always strive to achieve the best possible precision. From a practical point of view, more precision does not necessarily translate into better decision making. Despite the limitation in this section, we do not believe that we need more data with smart thermostats and LiDAR to recommend adding more vegetation in vulnerable neighbourhoods. We encourage the deployment of IoT technology that could improve early warning systems (Salim et al., 2023) and improve future studies, but this is not a limitation in implementing concrete adaptation solutions right now.

4.2. Strengths of this study

Despite the limitations that are inherent to the complexity of risk modelling, our study has several strengths.

Evaluating health impacts alone without connecting them with adaptation solutions is not sufficient for guiding decision making if we want to adapt efficiently to climate change (Muccione et al., 2024). Vulnerability assessments alone using social vulnerability indexes or any form of principal component analysis also often lack validation (Cheng et al., 2021) and agreement among experts (Estoque et al., 2023). They are also not useful tools for monitoring the efficiency of adaptation solutions. Therefore, there is an increasing need to use quantitative models to assess the risk of urban areas (Ye et al., 2021) and our study fills that gap. To the best of our knowledge, we are the first to perform a comprehensive risk assessment that includes projections that are based on the definition of IPCC AR6 (Pörtner et al., 2022) using GP.

Despite the Paris Agreement and a huge body of evidence-based recommendations, the gap between actions and scientific recommendations remains (Raiser et al., 2020). Therefore, it is necessary to

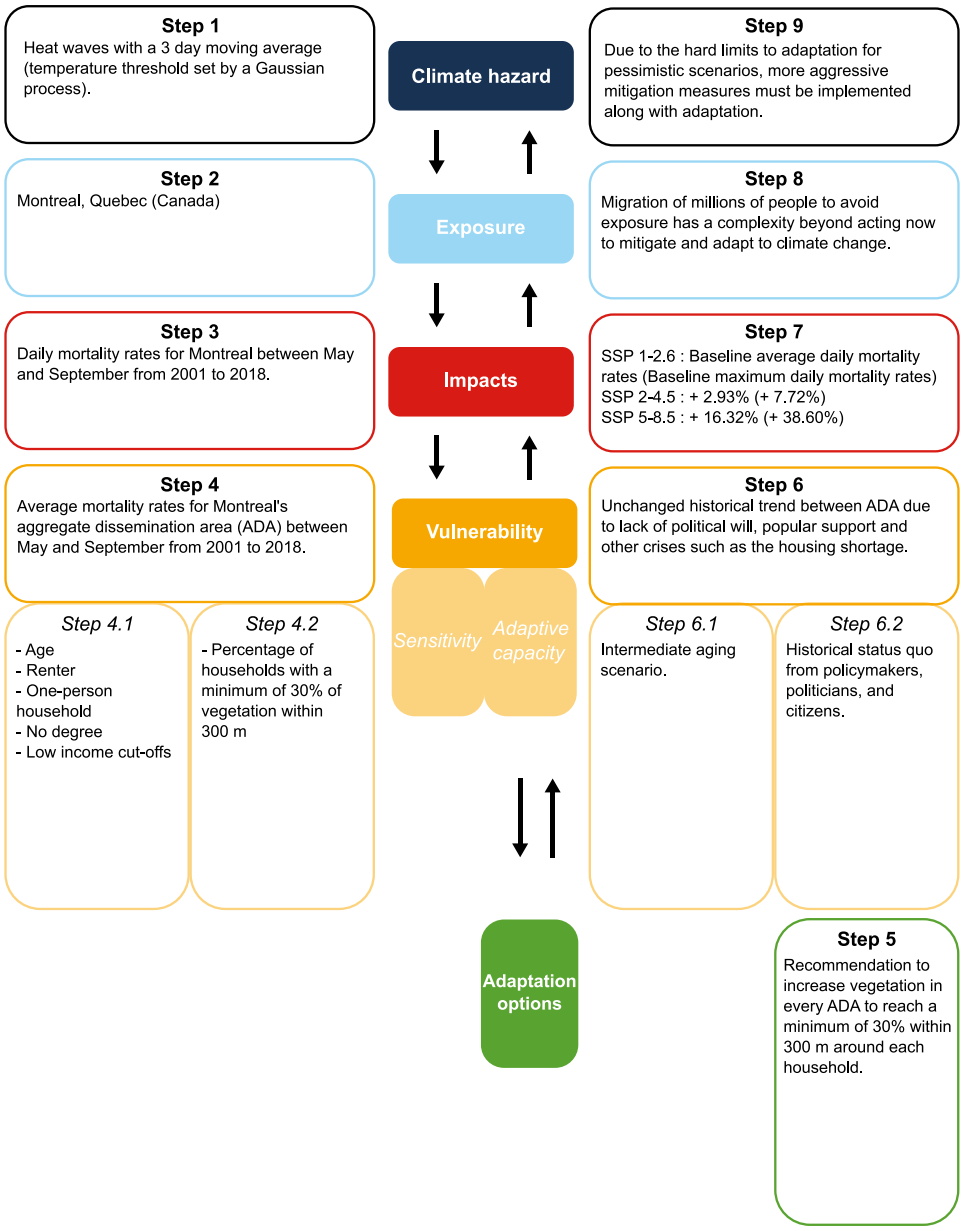

Fig. B.1. Example of a flowchart to guide decision making to manage climate risk based on exposure, impacts and vulnerability.

close this gap by ensuring that the results of the model can be easily translated into policies or can identify barriers and enablers (Hamilton, et al., 2021). A flowchart connecting the results of the intermediate aging scenario with the risk assessment framework is available in Appendix B. This can help inform the public and policymakers at a glance why adaptation is needed based on projected impacts, the challenge of adaptation, and the importance of increasing our effort to mitigate climate change. This flowchart can also be used to assess the risk qualitatively, as shown in Côté et al. (2024). Having a standardized framework that works with different levels of data quality can help in making a coherent adaptation strategy that can improve over time as more data are gathered and analysed.

4.3. Orientations for future research

Several questions still need to be investigated. Mortality during heat waves in an urban area is only a tiny fraction of adaptation to climate change. More hazards, impacts, and vulnerability profiles from different fields must be addressed to obtain a comprehensive view of global risk. We also need more research on the multi-risk compounding effect (Simpson, et al., 2021). Our GP model performance is adequate to provide a good insight on the risk faced by Montreal during heat waves, but the model could be improved to better reflect peak mortality during the worst historical heat waves and with advancement in projection techniques. Finally, it is still necessary to prove that this framework can really help implement and monitor adaptation options in a concrete situation that involves politicians and policymakers. This theoretical article is a first step before testing these ideas in the real world.

5. Conclusion

Despite a growing number of adaptation initiatives, the lack of validation for multiple risk and vulnerability frameworks in the scientific literature hampered action. The absence of standards makes it difficult to properly assess frameworks between each other and the adaptation options that result from them.

This article provided a comprehensive risk assessment of heat waves mortality in Montreal, including various aging and climate projections

(SSP1-2.6, SSP2-4.5 and SSP5-8.5). The use of GP that incorporates multiple socioeconomic and environmental variables fulfils the need for a quantitative model to better monitor and evaluate adaptation options. SHAP values help alleviate the black-box effect of the ML algorithm. The validation process shows that our model provides a good estimate for mortality at various temperature thresholds and can classify neighbourhoods based on how the mortality deviates from the regional mean. The impact assessment shows that Montreal will face increased summer mortality as the climate warms and the vulnerability assessment shows the need to increase the vegetation cover in vulnerable neighbourhoods.

A great deal of effort is put into modelling climate projections with initiatives such as the CMIP. Yet, risk models that include vulnerability are rare, despite being the most informative at guiding decision making. Heat waves in themselves are not necessarily a problem; it is their impacts on humans, ecosystems, and infrastructure that warrant actions. Therefore, more efforts should be made in the future to improve comprehensive risk modelling. More research is needed to validate which framework is best at closing the gap between science and political decisions.

CRediT authorship contribution statement

Jean-Nicolas Côté: Writing – review & editing, Writing – original draft, Visualization, Software, Methodology, Formal analysis, Conceptualization. **Elisabeth Levac:** Writing – review & editing, Supervision. **Mickaël Germain:** Writing – review & editing, Supervision. **Eric Lavigne:** Writing – review & editing, Supervision, Data curation.

Declaration of competing interest

The authors declare that they have no known competing financial interests or personal relationships that could have appeared to influence the work reported in this paper.

Acknowledgements

We wish to thank ClimateData.ca for providing the climate information that was used in this paper. ClimateData.ca was created through a collaboration between the Pacific Climate Impacts Consortium (PCIC, Victoria, BC), Ouranos Inc. (Montreal, QC), the Prairie Climate Centre (PCC, Winnipeg, MB), the Centre de Recherche Informatique de Montréal (CRIM) of Environment and Climate Change Canada (ECCC), and HabitatSeven (Ottawa, ON). The authors thank William F.J. Parsons for proofreading the article and the anonymous reviewers for their valuable insights.

Funding

This research did not receive any specific grants from funding agencies in the public, commercial, or not-for-profit sectors. It was conducted, in part, using the corresponding author's personal funding, together with contributions from a scientific research grant that is held by Mickaël Germain.

Appendix A. Risk assessment flowchart

See Fig. A.1.

Appendix B. Risk results flowchart example

See Fig. B.1.

Data availability

The data that has been used is confidential.

References

Ahn, Y., Tuholske, C., & Parks, R. M. (2024). Comparing approximated heat stress measures across the united states. *GeoHealth*, *8*(1), Article e2023GH000923. http://dx.doi.org/10.1029/2023GH000923.

Ali, S., Akhlaq, F., Imran, A. S., Kastrati, Z., Daudpota, S. M., & Moosa, M. (2023). The enlightening role of explainable artificial intelligence in medical & healthcare domains: A systematic literature review. *Computers in Biology and Medicine*, *166*, Article 107555. http://dx.doi.org/10.1016/j.compbiomed.2023.107555.

Allgaier, J., Mulansky, L., Draelos, R. L., & Pryss, R. (2023). How does the model make predictions? A systematic literature review on the explainability power of machine learning in healthcare. *Artificial Intelligence in Medicine*, *143*, Article 102616. http://dx.doi.org/10.1016/j.artmed.2023.102616.

Armenakis, C., & Nirupama, N. (2014). Urban impacts of ice storms: Toronto december 2013. *Natural Hazards*, *74*(2), 1291–1298. http://dx.doi.org/10.1007/s11069-014-1211-7.

Arsad, F. S., Hod, R., Ahmad, N., Ismail, R., Mohamed, N., Baharom, M., Osman, Y., Radi, M. F. M., & Tangang, F. (2022). The impact of heatwaves on mortality and morbidity and the associated vulnerability factors: A systematic review. *International Journal of Environmental Research and Public Health*, *19*(23), 16356. http://dx.doi.org/10.3390/ijerph192316356.

Baldwin, J. W., Benmarhnia, T., Ebi, K. L., Jay, O., Lutsko, N. J., & Vanos, J. K. (2023). Humidity's role in heat-related health outcomes: A heated debate. *Environmental Health Perspectives*, *131*(5), 55001. http://dx.doi.org/10.1289/EHP11807.

Barboza, E. P., Cirach, M., Khomenko, S., Iungman, T., Mueller, N., Barrera-Gómez, J., Rojas-Rueda, D., Kondo, M., & Nieuwenhuijsen, M. (2021). Green space and mortality in European cities: A health impact assessment study. *The Lancet Planetary Health*, *5*(10), e718–e730. http://dx.doi.org/10.1016/S2542-5196(21)00229-1.

Boudreault, J., Campagna, C., & Chebana, F. (2023). Machine and deep learning for modelling heat-health relationships. *Science of the Total Environment*, *892*, Article 164660. http://dx.doi.org/10.1016/j.scitotenv.2023.164660.

Boudreault, J., Campagna, C., & Chebana, F. (2024). Revisiting the importance of temperature, weather and air pollution variables in heat-mortality relationships with machine learning. *Environmental Science and Pollution Research*, *31*(9), 14059–14070. http://dx.doi.org/10.1007/s11356-024-31969-z.

Boudreault, J., Ruf, A., Campagna, C., & Chebana, F. (2024). Multi-region models built with machine and deep learning for predicting several heat-related health outcomes. *Sustainable Cities and Society*, Article 105785. http://dx.doi.org/10.1016/j.scs.2024.105785.

Buczynski, W., Cuzzolin, F., & Sahakian, B. (2021). A review of machine learning experiments in equity investment decision-making: Why most published research findings do not live up to their promise in real life. *International Journal of Data Science and Analysis*, *11*(3), 221–242. http://dx.doi.org/10.1007/s41060-021-00245-5.

Cannon, A. J., Sobie, S. R., & Murdock, T. Q. (2015). Bias correction of GCM precipitation by quantile mapping: How well do methods preserve changes in quantiles and extremes? *Journal of Climate*, *28*(17), 6938–6959. http://dx.doi.org/10.1175/JCLI-D-14-00754.1.

Chen, R.-C., Dewi, C., Huang, S.-W., & Caraka, R. E. (2020). Selecting critical features for data classification based on machine learning methods. *Journal of Big Data*, *7*(1), 1–26. http://dx.doi.org/10.1186/s40537-020-00327-4.

Chen, J., Jönsson, P., Tamura, M., Gu, Z., Matsushita, B., & Eklundh, L. (2004). A simple method for reconstructing a high-quality NDVI time-series data set based on the Savitzky–Golay filter. *Remote Sensing of Environment*, *91*(3), 332–344. http://dx.doi.org/10.1016/j.rse.2004.03.014.

Cheng, W., Li, D., Liu, Z., & Brown, R. D. (2021). Approaches for identifying heat-vulnerable populations and locations: A systematic review. *Science of the Total Environment*, *799*, Article 149417. http://dx.doi.org/10.1016/j.scitotenv.2021.149417.

Cheng, J., Xu, Z., Bambrick, H., Su, H., Tong, S., & Hu, W. (2018). Heatwave and elderly mortality: An evaluation of death burden and health costs considering short-term mortality displacement. *Environment International*, *115*, 334–342. http://dx.doi.org/10.1016/j.envint.2018.03.041.

Choi, H. M., Lee, W., Roye, D., Heo, S., Urban, A., Entezari, A., Vicedo-Cabrera, A. M., Zanobetti, A., Gasparrini, A., Analitis, A., Tobias, A., Armstrong, B., Forsberg, B., Íñiguez, C., Åström, C., Indermitte, E., Lavigne, E., Mayvaneh, F., Acquaotta, F., ... Bell, M. L. (2022). Effect modification of greenness on the association between heat and mortality: A multi-city multi-country study. *eBioMedicine*, *84*, Article 104251. http://dx.doi.org/10.1016/j.ebiom.2022.104251.

Chow, K. K. C., Sankaré, H., Diaconescu, E. P., Murdock, T. Q., & Cannon, A. J. (2024). Bias-adjusted and downscaled humidex projections for heat preparedness and adaptation in Canada. *Geoscience Data Journal*, *n/a*(n/a), http://dx.doi.org/10.1002/gdj3.241.

ClimateData. ca (2024). CMIP6 dataset. URL https://climatedata.ca/.

Conti, A., Valente, M., Paganini, M., Farsoni, M., Ragazzoni, L., & Barone-Adesi, F. (2022). Knowledge gaps and research priorities on the health effects of heatwaves: A systematic review of reviews. *International Journal of Environmental Research and Public Health*, *19*(10), 5887. http://dx.doi.org/10.3390/ijerph19105887.

Cordiner, R., Wan, K., Hajat, S., & Macintyre, H. L. (2024). Accounting for adaptation when projecting climate change impacts on health: A review of temperature-related health impacts. *Environment International*, *188*, Article 108761. http://dx.doi.org/10.1016/j.envint.2024.108761.

Côté, J.-N., Germain, M., Levac, E., & Lavigne, E. (2024). Vulnerability assessment of heat waves within a risk framework using artificial intelligence. *Science of the Total Environment*, *912*, Article 169355. http://dx.doi.org/10.1016/j.scitotenv.2023.169355.

Dardir, M., Berardi, U., & Wilson, J. (2023). Health-informed predictive regression for statistical-simulation decision-making in urban heat mitigation. *Sustainable Cities and Society*, *98*, Article 104853. http://dx.doi.org/10.1016/j.scs.2023.104853.

de Schrijver, E., Folly, C. L., Schneider, R., Royé, D., Franco, O. H., Gasparrini, A., & Vicedo-Cabrera, A. M. (2021). A comparative analysis of the temperature-mortality risks using different weather datasets across heterogeneous regions. *GeoHealth*, *5*(5), http://dx.doi.org/10.1029/2020GH000363.

Dhamodharavadhani, S., & Rathipriya, R. (2021). COVID-19 mortality rate prediction for India using statistical neural networks and Gaussian process regression model. *African Health Sciences*, *21*(1), 194–206. http://dx.doi.org/10.4314/ahs.v21i1.26.

Ding, T., Li, H., Tan, R., & Zhao, X. (2023). How does geopolitical risk affect carbon emissions?: An empirical study from the perspective of mineral resources extraction in OECD countries. *Resources Policy*, *85*, Article 103983. http://dx.doi.org/10.1016/j.resourpol.2023.103983.

Djulbegovic, B., & Guyatt, G. H. (2017). Progress in evidence-based medicine: A quarter century on. *The Lancet*, *390*(10092), 415–423. http://dx.doi.org/10.1016/S0140-6736(16)31592-6.

Dodman, D., Hayward, B., Pelling, M., Castan Broto, V., Chow, W., Chu, E., Dawson, R., Khirfan, L., McPhearson, T., Prakash, A., Zheng, Y., & Ziervogel, G. (2022). Cities, settlements and key infrastructure. In H. O. Pörtner, D. C. Roberts, M. Tignor, E. S. Poloczanska, K. Mintenbeck, A. Alegría, M. Craig, S. Langsdorf, S. Löschke, V. Möller, A. Okem, & B. Rama (Eds.), *Climate change 2022: impacts, adaptation and vulnerability. contribution of working group II to the sixth assessment report of the intergovernmental panel on climate change* (pp. 907–1040). Cambridge, UK and New York, USA: Cambridge University Press, http://dx.doi.org/10.1017/9781009325844.008.907.

Dominski, F. H., Lorenzetti Branco, J. H., Buonanno, G., Stabile, L., Gameiro da Silva, M., & Andrade, A. (2021). Effects of air pollution on health: A mapping review of systematic reviews and meta-analyses. *Environmental Research*, *201*, Article 111487. http://dx.doi.org/10.1016/j.envres.2021.111487.

Doyon, B., Bélanger, D., & Gosselin, P. (2008). The potential impact of climate change on annual and seasonal mortality for three cities in Québec, Canada. *International Journal of Health Geographics*, *7*(1), 23. http://dx.doi.org/10.1186/1476-072X-7-23.

Duvenaud, D. K. (2014). *Automatic model construction with Gaussian processes* (Ph.D. thesis), University of Cambridge.

den Elzen, M. G. J., Dafnomilis, I., Forsell, N., Fragkos, P., Fragkiadakis, K., Höhne, N., Kuramochi, T., Nascimento, L., Roelfsema, M., van Soest, H., & Sperling, F. (2022). Updated nationally determined contributions collectively raise ambition levels but need strengthening further to keep Paris goals within reach. *Mitigaion Adapting Strategies of Global Change*, *27*(5), 33. http://dx.doi.org/10.1007/s11027-022-10008-7.

Esperon-Rodriguez, M., Rymer, P. D., Power, S. A., Barton, D. N., Cariñanos, P., Dobbs, C., Eleuterio, A. A., Escobedo, F. J., Hauer, R., Hermy, M., Jahani, A., Onyekwelu, J. C., Östberg, J., Pataki, D., Randrup, T. B., Rasmussen, T. r., Roman, L. A., Russo, A., Shackleton, C., ... Tjoelker, M. G. (2022). Assessing climate risk to support urban forests in a changing climate. *Plants, People, Planet*, *4*(3), 201–213. http://dx.doi.org/10.1002/ppp3.10240.

Estoque, R. C., Ishtiaque, A., Parajuli, J., Athukorala, D., Rabby, Y. W., & Ooba, M. (2023). Has the IPCC's revised vulnerability concept been well adopted? *Ambio*, *52*(2), 376–389. http://dx.doi.org/10.1007/s13280-022-01806-z.

Farhan, B. Y. (2024). Canada's leadership and housing affordability: Evidence from the Canadian real estate market. *Journal of Urban Management*, *13*(1), 52–61. http://dx.doi.org/10.1016/j.jum.2023.11.001.

Gao, K., Feng, J., & Santamouris, M. (2024). Are grand tree planting initiatives meeting expectations in mitigating urban overheating during heat waves? *Sustainable Cities and Society*, *113*, Article 105671. http://dx.doi.org/10.1016/j.scs.2024.105671.

Garschagen, M., Doshi, D., Reith, J., & Hagenlocher, M. (2021). Global patterns of disaster and climate risk—an analysis of the consistency of leading index-based assessments and their results. *Climatic Change*, *169*(1), 11. http://dx.doi.org/10.1007/s10584-021-03209-7.

Gasparrini, A., & Leone, M. (2014). Attributable risk from distributed lag models. *BMC Medical Research Methodology*, *14*(1), 55. http://dx.doi.org/10.1186/1471-2288-14-55.

Goodman, Z. T., Stamatis, C. A., Stoler, J., Emrich, C. T., & Llabre, M. M. (2021). Methodological challenges to confirmatory latent variable models of social vulnerability. *Natural Hazards*, http://dx.doi.org/10.1007/s11069-021-04563-6.

Gorelick, N., Hancher, M., Dixon, M., Ilyushchenko, S., Thau, D., & Moore, R. (2017). Google earth engine: Planetary-scale geospatial analysis for everyone. In *Big remotely sensed data: tools, applications and experiences*: *Remote Sensing of Environment*, In *Big remotely sensed data: tools, applications and experiences*: *202*, 18–27.http://dx.doi.org/10.1016/j.rse.2017.06.031,

Guo, Y., Gasparrini, A., Armstrong, B. G., Tawatsupa, B., Tobias, A., Lavigne, E., Coelho, M. d. Z. S., Pan, X., Kim, H., Hashizume, M., Honda, Y., Guo, Y.-L. L., Wu, C.-F., Zanobetti, A., Schwartz, J. D., Bell, M. L., Scortichini, M., Michelozzi, P., Punnasiri, K., ... Tong, S. (2017). Heat wave and mortality: A multicountry, Multicommunity Study. *Environmental Health Perspectives*, *125*(8), Article 087006. http://dx.doi.org/10.1289/EHP1026.

Hamilton, I., Kennard, H., McGushin, A., Höglund-Isaksson, L., Kiesewetter, G., Lott, M., Milner, J., Purohit, P., Rafaj, P., Sharma, R., Springmann, M., Woodcock, J., & Watts, N. (2021). The public health implications of the Paris agreement: A modelling study. *The Lancet Planetary Health*, *5*(2), e74–e83. http://dx.doi.org/10.1016/S2542-5196(20)30249-7.

Hammond, W. M., Williams, A. P., Abatzoglou, J. T., Adams, H. D., Klein, T., López, R., Sáenz-Romero, C., Hartmann, H., Breshears, D. D., & Allen, C. D. (2022). Global field observations of tree die-off reveal hotter-drought fingerprint for Earth's forests. *Nature Communication*, *13*(1), 1761. http://dx.doi.org/10.1038/s41467-022-29289-2.

Hanna, E. G., & Tait, P. W. (2015). Limitations to thermoregulation and acclimatization challenge human adaptation to global warming. *International Journal of Environmental Research and Public Health*, *12*(7), 8034–8074. http://dx.doi.org/10.3390/ijerph120708034.

Harris, C. R., Millman, K. J., van der Walt, S. J., Gommers, R., Virtanen, P., Cournapeau, D., Wieser, E., Taylor, J., Berg, S., Smith, N. J., Kern, R., Picus, M., Hoyer, S., van Kerkwijk, M. H., Brett, M., Haldane, A., del Río, J. F., Wiebe, M., Peterson, P., ... Oliphant, T. E. (2020). Array programming with NumPy. *Nature*, *585*(7825), 357–362. http://dx.doi.org/10.1038/s41586-020-2649-2.

Hebbern, C., Gosselin, P., Chen, K., Chen, H., Cakmak, S., MacDonald, M., Chagnon, J., Dion, P., Martel, L., & Lavigne, E. (2023). Future temperature-related excess mortality under climate change and population aging scenarios in Canada. *Canadian Journal of Public Health. Revue Canadienne de Sante Publique*, *114*(5), 726–736. http://dx.doi.org/10.17269/s41997-023-00782-5.

Heinl, M., Hammerle, A., Tappeiner, U., & Leitinger, G. (2015). Determinants of urban–rural land surface temperature differences – A landscape scale perspective. *Landscape and Urban Planning*, *134*, 33–42. http://dx.doi.org/10.1016/j.landurbplan.2014.10.003.

Hunter, J. D. (2007). Matplotlib: A 2D graphics environment. *Computing in Science & Engineering*, *9*(3), 90–95. http://dx.doi.org/10.1109/MCSE.2007.55.

Institut de la statistique du Québec (2024). Espérance de vie à la naissance selon le sexe, régions administratives du Québec. URL https://statistique.quebec.ca/fr/produit/publication/esperance-vie-naissance-selon-sexe-regions-administratives-quebec.

Jewell, J., & Cherp, A. (2020). On the political feasibility of climate change mitigation pathways: Is it too late to keep warming below 1.5°C? *Wiley Interdisciplinary Reviews: Climate Change*, *11*(1), http://dx.doi.org/10.1002/wcc.621.

Ju, Y., Dronova, I., Ma, Q., Lin, J., Moran, M. R., Gouveia, N., Hu, H., Yin, H., & Shang, H. (2024). Assessing normalized difference vegetation index as a proxy of urban greenspace exposure. *Urban Forestry & Urban Greening*, *99*, Article 128454. http://dx.doi.org/10.1016/j.ufug.2024.128454.

Kanti, F. S., Alari, A., Chaix, B., & Benmarhnia, T. (2022). Comparison of various heat waves definitions and the burden of heat-related mortality in France: implications for existing early warning systems. *Environmental Research*, *215*, Article 114359. http://dx.doi.org/10.1016/j.envres.2022.114359.

Karanja, J., & Kiage, L. (2021). Perspectives on spatial representation of urban heat vulnerability. *Science of the Total Environment*, *774*, Article 145634. http://dx.doi.org/10.1016/j.scitotenv.2021.145634.

Katal, A., Leroyer, S., Zou, J., Nikiema, O., Albettar, M., Belair, S., & Wang, L. L. (2023). Outdoor heat stress assessment using an integrated multi-scale numerical weather prediction system: A case study of a heatwave in montreal. *Science of the Total Environment*, *865*, Article 161276. http://dx.doi.org/10.1016/j.scitotenv.2022.161276.

Kelly, C. J., Karthikesalingam, A., Suleyman, M., Corrado, G., & King, D. (2019). Key challenges for delivering clinical impact with artificial intelligence. *BMC Medicine*, *17*(1), 1–9. http://dx.doi.org/10.1186/s12916-019-1426-2.

Kemp, L., Xu, C., Depledge, J., Ebi, K. L., Gibbins, G., Kohler, T. A., Rockström, J., Scheffer, M., Schellnhuber, H. J., Steffen, W., & Lenton, T. M. (2022). Climate endgame: Exploring catastrophic climate change scenarios. *Proceedings of the National Academy of Sciences*, *119*(34), Article e2108146119. http://dx.doi.org/10.1073/pnas.2108146119.

Kuhlicke, C., Madruga de Brito, M., Bartkowski, B., Botzen, W., Doğulu, C., Han, S., Hudson, P., Nuray Karanci, A., Klassert, C. J., Otto, D., Scolobig, A., Moreno Soares, T., & Rufat, S. (2023). Spinning in circles? A systematic review on the role of theory in social vulnerability, resilience and adaptation research. *Global Environmental Change*, *80*, Article 102672. http://dx.doi.org/10.1016/j.gloenvcha.2023.102672.

Kwakkenbos, L., Imran, M., McCall, S. J., McCord, K. A., Fröbert, O., Hemkens, L. G., Zwarenstein, M., Relton, C., Rice, D. B., Langan, S. M., Benchimol, E. I., Thabane, L., Campbell, M. K., Sampson, M., Erlinge, D., Verkooijen, H. M., Moher, D., Boutron, I., Ravaud, P., ... Thombs, B. D. (2021). CONSORT extension for the reporting of randomised controlled trials conducted using cohorts and routinely collected data (CONSORT-ROUTINE): Checklist with explanation and elaboration. *BMJ*, *373*, n857. http://dx.doi.org/10.1136/bmj.n857.

Li, J., Woodward, A., Hou, X.-Y., Zhu, T., Zhang, J., Brown, H., Yang, J., Qin, R., Gao, J., Gu, S., Li, J., Xu, L., Liu, X., & Liu, Q. (2017). Modification of the effects of air pollutants on mortality by temperature: A systematic review and meta-analysis. *Science of the Total Environment*, *575*, 1556–1570. http://dx.doi.org/10.1016/j.scitotenv.2016.10.070.

Li, F., Yigitcanlar, T., Nepal, M., Thanh, K. N., & Dur, F. (2022). Understanding urban heat vulnerability assessment methods: A PRISMA review. *Energies*, *15*(19), 6998. http://dx.doi.org/10.3390/en15196998.

Li, F., Yigitcanlar, T., Nepal, M., Thanh, K. N., & Dur, F. (2024). A novel urban heat vulnerability analysis: Integrating machine learning and remote sensing for enhanced insights. *Remote Sensing*, *16*(16), 3032. http://dx.doi.org/10.3390/rs16163032.

Liu, X.-X., Ma, X.-L., Huang, W.-Z., Luo, Y.-N., He, C.-J., Zhong, X.-M., Dadvand, P., Browning, M. H. E. M., Li, L., Zou, X.-G., Dong, G.-H., & Yang, B.-Y. (2022). Green space and cardiovascular disease: A systematic review with meta-analysis. *Environmental Pollution*, *301*, Article 118990. http://dx.doi.org/10.1016/j.envpol.2022.118990.

Liu, H., Ong, Y.-S., Shen, X., & Cai, J. (2020). When Gaussian process meets big data: A review of scalable GPs. *IEEE Transactions on Neural Networks and Learning Systems*, *31*(11), 4405–4423. http://dx.doi.org/10.1109/TNNLS.2019.2957109.

Liu, D., Zhou, R., Ma, Q., He, T., Fang, X., Xiao, L., Hu, Y., Li, J., Shao, L., & Gao, J. (2024). Spatio-temporal patterns and population exposure risks of urban heat island in megacity Shanghai, China. *Sustainable Cities and Society*, *108*, Article 105500. http://dx.doi.org/10.1016/j.scs.2024.105500.

Lo, Y. T. E., Mitchell, D. M., Buzan, J. R., Zscheischler, J., Schneider, R., Mistry, M. N., Kyselý, J., Lavigne, E., da Silva, S. P., Royé, D., Urban, A. s., Armstrong, B., Network, Gasparrini, A., & Vicedo-Cabrera, A. M. (2023). Optimal heat stress metric for modelling heat-related mortality varies from country to country. *International Journal of Climatology*, *43*(12), 5553–5568. http://dx.doi.org/10.1002/joc.8160.

Loh, H. W., Ooi, C. P., Seoni, S., Barua, P. D., Molinari, F., & Acharya, U. R. (2022). Application of explainable artificial intelligence for healthcare: A systematic review of the last decade (2011–2022). *Computer Methods and Programs in Biomedicine*, *226*, Article 107161. http://dx.doi.org/10.1016/j.cmpb.2022.107161.

Ludkovski, M., Risk, J., & Zail, H. (2018). Gaussian process models for mortality rates and improvment factors. *ASTIN Bulletin: The Journal of the IAA*, *48*(3), 1307–1347. http://dx.doi.org/10.1017/asb.2018.24.

Lundberg, S. M., & Lee, S.-I. (2017). A unified approach to interpreting model predictions. In I. Guyon, U. V. Luxburg, S. Bengio, H. Wallach, R. Fergus, S. Vishwanathan, & R. Garnett (Eds.), *Advances in neural information processing systems 30* (pp. 4765–4774). Curran Associates, Inc., URL http://papers.nips.cc/paper/7062-a-unified-approach-to-interpreting-model-predictions.pdf.

Mah, J. C., Penwarden, J. L., Pott, H., Theou, O., & Andrew, M. K. (2023). Social vulnerability indices: A scoping review. *BMC Public Health*, *23*(1), 1–11. http://dx.doi.org/10.1186/s12889-023-16097-6.

Marchin, R. M., Esperon-Rodriguez, M., Tjoelker, M. G., & Ellsworth, D. S. (2022). Crown dieback and mortality of urban trees linked to heatwaves during extreme drought. *Science of the Total Environment*, *850*, Article 157915. http://dx.doi.org/10.1016/j.scitotenv.2022.157915.

Marrel, A., & Iooss, B. (2024). Probabilistic surrogate modeling by Gaussian process: A review on recent insights in estimation and validation. *Reliability Engineering & System Safety*, *247*, Article 110094. http://dx.doi.org/10.1016/j.ress.2024.110094.

Martin, S. L., Cakmak, S., Hebbern, C. A., Avramescu, M.-L., & Tremblay, N. (2012). Climate change and future temperature-related mortality in 15 Canadian cities. *International Journal of Biometeorology*, *56*(4), 605–619. http://dx.doi.org/10.1007/s00484-011-0449-y.

Matthews, A. G. d. G., van der Wilk, M., Nickson, T., Fujii, K., Boukouvalas, A., León-Villagrá, P., Ghahramani, Z., & Hensman, J. (2016). GPflow: A Gaussian process library using tensorflow. (arXiv:1610.08733), http://dx.doi.org/10.48550/arXiv.1610.08733, arXiv:1610.08733.

McKenney, D. W., Hutchinson, M. F., Papadopol, P., Lawrence, K., Pedlar, J., Campbell, K., Milewska, E., Hopkinson, R. F., Price, D., & Owen, T. (2011). Customized spatial climate models for North America. *Bulletin of the American Meteorological Society*, *92*(12), 1611–1622. http://dx.doi.org/10.1175/2011BAMS3132.1.

McKinney, W. (2010). Data structures for statistical computing in Python. In S. van der Walt, & J. Millman (Eds.), *Proceedings of the 9th python in science conference* (pp. 56–61). http://dx.doi.org/10.25080/Majora-92bf1922-00a.

Ministère de la Santé et des Services sociaux (MSSSS) (2023). RED/D - Sources de données et métadonnées - professionnels de la santé - MSSS. URL https://www.msss.gouv.qc.ca/professionnels/documentation-sources-de-donnees-et-indicateurs/sources-de-donnees-et-metadonnees/red-d/.

Ministère des ressources naturelles et des forêts (2024). Adresses Québec. URL https://www.donneesquebec.ca/recherche/dataset/adresses-quebec.

Monod, M., Blenkinsop, A., Brizzi, A., Chen, Y., Perello, C. C. C., Jogarah, V., Wang, Y., Flaxman, S., Bhatt, S., & Ratmann, O. (2023). Regularised B-splines projected Gaussian process priors to estimate time-trends in age-specific COVID-19 deaths. *Bayesian Analysis*, *18*(3), 957–987. http://dx.doi.org/10.1214/22-BA1334.

Muccione, V., Biesbroek, R., Harper, S., & Haasnoot, M. (2024). Towards a more integrated research framework for heat-related health risks and adaptation. *The Lancet Planetary Health*, *8*(1), e61–e67. http://dx.doi.org/10.1016/S2542-5196(23)00254-1.

Oetomo, A., Jalali, N., Costa, P. D. P., & Morita, P. P. (2022). Indoor temperatures in the 2018 heat wave in Quebec, Canada: Exploratory study using ecobee smart thermostats. *JMIR Formative Research*, *6*(5), Article e34104. http://dx.doi.org/10.2196/34104.

O'Neill, B. C., Kriegler, E., Ebi, K. L., Kemp-Benedict, E., Riahi, K., Rothman, D. S., van Ruijven, B. J., van Vuuren, D. P., Birkmann, J., Kok, K., Levy, M., & Solecki, W. (2017). The roads ahead: narratives for shared socioeconomic pathways describing world futures in the 21st century. *Global Environmental Change*, *42*, 169–180. http://dx.doi.org/10.1016/j.gloenvcha.2015.01.004.

Orellano, P., Reynoso, J., Quaranta, N., Bardach, A., & Ciapponi, A. (2020). Short-term exposure to particulate matter (PM10 and PM2.5), nitrogen dioxide (NO2), and ozone (O3) and all-cause and cause-specific mortality: systematic review and *Meta*-analysis. *Environment International*, *142*, Article 105876. http://dx.doi.org/10.1016/j.envint.2020.105876.

Oulahen, G., Klein, Y., Mortsch, L., O'Connell, E., & Harford, D. (2018). Barriers and drivers of planning for Climate Change Adaptation across three levels of government in Canada. *Planning Theory & Practice*, URL https://www.tandfonline.com/doi/abs/10.1080/14649357.2018.1481993.

Painter, M. A., Shah, S. H., Damestoit, G. C., Khalid, F., Prudencio, W., Chisty, M. A., Tormos-Aponte, F., & Wilhelmi, O. (2024). A systematic scoping review of the social vulnerability index as applied to natural hazards. *Natural Hazards*, http://dx.doi.org/10.1007/s11069-023-06378-z.

Park, M.-S., & Baek, K. (2023). Quality management system for an IoT meteorological sensor network—Application to smart seoul data of things (S-DoT). *Sensors*, *23*(5), 2384. http://dx.doi.org/10.3390/s23052384.

Pascal, M., Goria, S., Wagner, V., Sabastia, M., Guillet, A., Cordeau, E., Mauclair, C., & Host, S. (2021). Greening is a promising but likely insufficient adaptation strategy to limit the health impacts of extreme heat. *Environment International*, *151*, Article 106441. http://dx.doi.org/10.1016/j.envint.2021.106441.

Picketts, I. M. (2018). The best laid plans: Impacts of politics on local climate change adaptation. *Environmental Science & Policy*, *87*, 26–32. http://dx.doi.org/10.1016/j.envsci.2018.05.017.

Pörtner, H.-O., Roberts, D., Adams, H., Adelekan, I., Adler, C., Adrian, R., Aldunce, P., Ali, E., Begum, R. A., Friedl, B. B., Kerr, R. B., Biesbroek, R., Birkmann, J., Bowen, K., Caretta, M., Carnicer, J., Castellanos, E., Cheong, T., Chow, W., ... Ibrahim, Z. Z. (2022). *Technical summary*, *Climate change 2022: Impacts, adaptation and vulnerability* (pp. 37–118). Cambridge, UK and New York, USA: Cambridge University Press, http://dx.doi.org/10.1017/9781009325844.002.

QGIS Development Team (2024). QGIS. URL https://www.qgis.org.

Rachid, A., & Qureshi, A. M. (2023). Sensitivity analysis of heat stress indices. *Climate*, *11*(9), 181. http://dx.doi.org/10.3390/cli11090181.

Raiser, K., Kornek, U., Flachsland, C., & Lamb, W. F. (2020). Is the Paris agreement effective? A systematic map of the evidence. *Environmental Research Letters*, *15*(8), Article 083006. http://dx.doi.org/10.1088/1748-9326/ab865c.

Rajagopalan, P., Andamon, M. M., & Paolini, R. (2020). Investigating thermal comfort and energy impact through microclimate monitoring- a citizen science approach. *Energy and Buildings*, *229*, Article 110526. http://dx.doi.org/10.1016/j.enbuild.2020.110526.

Raška, P., Dolejš, M., Pacina, J., Popelka, J., Píša, J., & Rybová, K. (2020). Review of current approaches to spatially explicit urban vulnerability assessments: Hazard complexity, data sources, and cartographic representations. *GeoScape*, *14*(1), 47–61. http://dx.doi.org/10.2478/geosc-2020-0005.

Rasmussen, C. E., & Williams, C. K. I. (2006). *Adaptive computation and machine learning: vol. 2, Gaussian Processes for Machine Learning*. Cambridge, Mass: MIT Press.

Roberts, S., Osborne, M., Ebden, M., Reece, S., Gibson, N., & Aigrain, S. (2013). Gaussian processes for time-series modelling. *Phil. Trans. R. Soc. A.*, *371*(1984), Article 20110550. http://dx.doi.org/10.1098/rsta.2011.0550.

Rojas-Rueda, D., Nieuwenhuijsen, M. J., Gascon, M., Perez-Leon, D., & Mudu, P. (2019). Green spaces and mortality: A systematic review and meta-analysis of cohort studies. *The Lancet Planetary Health*, *3*(11), e469–e477. http://dx.doi.org/10.1016/S2542-5196(19)30215-3.

Salim, S., Zakir Hussain, I., Kaur, J., & Morita, P. P. (2023). An early warning system for air pollution surveillance: A big data framework to monitoring risks associated with air pollution. In *2023 IEEE international conference on big data (bigData)* (pp. 3371–3374). http://dx.doi.org/10.1109/BigData59044.2023.10386185.

Schulz, E., Speekenbrink, M., & Krause, A. (2018). A tutorial on Gaussian process regression: Modelling, exploring, and exploiting functions. *Journal of Mathematical Psychology*, *85*, 1–16. http://dx.doi.org/10.1016/j.jmp.2018.03.001.

Seong, K., Jiao, J., Mandalapu, A., & Niyogi, D. (2024). Spatio-temporal patterns of heat index and heat-related emergency medical services (EMS). *Sustainable Cities and Society*, *111*, Article 105562. http://dx.doi.org/10.1016/j.scs.2024.105562.

Sharifi, A., Pathak, M., Joshi, C., & He, B.-J. (2021). A systematic review of the health co-benefits of urban climate change adaptation. *Sustainable Cities and Society*, *74*, Article 103190. http://dx.doi.org/10.1016/j.scs.2021.103190.

Sheehan, T., Min, E., & Hess, J. (2023). A comparison of hazard vulnerability indexes for Washington State. *Journal of Homeland Security and Emergency Management*, http://dx.doi.org/10.1515/jhsem-2021-0066.

Simpson, C. H., Brousse, O., Ebi, K. L., & Heaviside, C. (2023). Commonly used indices disagree about the effect of moisture on heat stress. *npj Climate of Atmosphere Science*, *6*(1), 1–7. http://dx.doi.org/10.1038/s41612-023-00408-0.

Simpson, N. P., Mach, K. J., Constable, A., Hess, J., Hogarth, R., Howden, M., Lawrence, J., Lempert, R. J., Muccione, V., Mackey, B., New, M. G., O'Neill, B., Otto, F., Pörtner, H.-O., Reisinger, A., Roberts, D., Schmidt, D. N., Seneviratne, S., Strongin, S., ... Trisos, C. H. (2021). A framework for complex climate change risk assessment. *One Earth*, *4*(4), 489–501. http://dx.doi.org/10.1016/j.oneear.2021.03.005.

Singh, N., Areal, A. T., Breitner, S., Zhang, S., Agewall, S., Schikowski, T., & Schneider, A. (2024). Heat and cardiovascular mortality: An epidemiological perspective. *Circulation Research*, *134*(9), 1098–1112. http://dx.doi.org/10.1161/CIRCRESAHA.123.323615.

Sinha, P., Coville, R. C., Hirabayashi, S., Lim, B., Endreny, T. A., & Nowak, D. J. (2022). Variation in estimates of heat-related mortality reduction due to tree cover in U.S. cities. *Journal of Environmental Management*, *301*, Article 113751. http://dx.doi.org/10.1016/j.jenvman.2021.113751.

Sobie, S. R., Ouali, D., Curry, C. L., & Zwiers, F. W. (2024). Multivariate Canadian downscaled climate scenarios for CMIP6 (CanDCS-M6). *Geoscience Data Journal*, *n/a*(n/a), http://dx.doi.org/10.1002/gdj3.257.

Spangler, K. R., Adams, Q. H., Hu, J. K., Braun, D., Weinberger, K. R., Dominici, F., & Wellenius, G. A. (2023). Does choice of outdoor heat metric affect heat-related epidemiologic analyses in the US Medicare population? *Environmental Epidemiology*, *7*(4), Article e261. http://dx.doi.org/10.1097/EE9.0000000000000261.

Spangler, K. R., Weinberger, K. R., & Wellenius, G. A. (2019). Suitability of gridded climate datasets for use in environmental epidemiology. *Journal of Export Sciene and Environment Epidemiology*, *29*(6), 777–789. http://dx.doi.org/10.1038/s41370-018-0105-2.

Spielman, S. E., Tuccillo, J., Folch, D. C., Schweikert, A., Davies, R., Wood, N., & Tate, E. (2020). Evaluating social vulnerability indicators: Criteria and their application to the social vulnerability index. *Natural Hazards*, *100*(1), 417–436. http://dx.doi.org/10.1007/s11069-019-03820-z.

Stafoggia, M., Michelozzi, P., Schneider, A., Armstrong, B., Scortichini, M., Rai, M., Achilleos, S., Alahmad, B., Analitis, A., Åström, C., Bell, M. L., Calleja, N., Krage Carlsen, H., Carrasco, G., Paul Cauchi, J., DSZS Coelho, M., Correa, P. M., Diaz, M. H., Entezari, A., ... de' Donato, F. K. (2023). Joint effect of heat and air pollution on mortality in 620 cities of 36 countries. *Environment International*, *181*, Article 108258. http://dx.doi.org/10.1016/j.envint.2023.108258.

Statistics Canada (2001). Profile for Canada, provinces, territories, census divisions, census subdivisions and dissemination areas, 2001 census. catalogue no. 95F0495X2001002. URL https://www150.statcan.gc.ca/n1/en/catalogue/95F0495X2001002.

Statistics Canada (2006). Profile for Canada, provinces, territories, census divisions, census subdivisions and dissemination areas, 2006 census. catalogue no. 94-581-XCB2006002. URL https://www12.statcan.gc.ca/census-recensement/2006/dp-pd/prof/rel/index-eng.cfm.

Statistics Canada (2011). Profile for Canada, provinces, territories, census divisions, census subdivisions and dissemination areas, 2011 census. catalogue no. 98-316-XWF2011001-1501. URL https://www12.statcan.gc.ca/census-recensement/2011/dp-pd/prof/details/download-telecharger/comprehensive/comp-csv-tab-dwnld-tlchrgr.cfm?Lang=E#tabs2011.

Statistics Canada (2016). Dictionary, census of population, 2016, catalogue no. 98-301-X2016001. URL https://www12.statcan.gc.ca/census-recensement/2016/ref/dict/98-301-x2016001-eng.pdf.

Statistics Canada (2016). Profile for Canada, provinces, territories, census divisions, census subdivisions and dissemination areas, 2016 census. catalogue no. 98-401-X2016044. URL https://www12.statcan.gc.ca/census-recensement/2016/dp-pd/prof/details/download-telecharger/comp/page_dl-tc.cfm?Lang=E.

Statistics Canada (2018). Postal code OM conversion file plus (PCCF+). URL https://www150.statcan.gc.ca/n1/en/catalogue/82F0086X.

Statistics Canada (2021). Profile for Canada, provinces, territories, census divisions, census subdivisions and dissemination areas, 2016 census. catalogue no. 98-401-X2021006. URL https://www12.statcan.gc.ca/census-recensement/2021/dp-pd/prof/details/download-telecharger.cfm?Lang=E.

Statistics Canada (2022). Population projections for Canada (2021 to 2068), provinces and territories (2021 to 2043). URL https://www150.statcan.gc.ca/n1/pub/91-520-x/91-520-x2022001-eng.htm.

Stoddard, I., Anderson, K., Capstick, S., Carton, W., Depledge, J., Facer, K., Gough, C., Hache, F., Hoolohan, C., Hultman, M., Hällström, N., Kartha, S., Klinsky, S., Kuchler, M., Lövbrand, E., Nasiritousi, N., Newell, P., Peters, G. P., Sokona, Y., ... Williams, M. (2021). Three decades of climate mitigation: Why haven't we bent the global emissions curve? *Annual Review of Environment and Resources*, *46*(1), 653–689. http://dx.doi.org/10.1146/annurev-environ-012220-011104.

Sützl, B. S., Strebel, D. A., Rubin, A., Wen, J., & Carmeliet, J. (2024). Urban morphology clustering analysis to identify heat-prone neighbourhoods in cities. *Sustainable Cities and Society*, *107*, Article 105360. http://dx.doi.org/10.1016/j.scs.2024.105360.

Thomas, N., Ebelt, S. T., Newman, A. J., Scovronick, N., D'Souza, R. R., Moss, S. E., Warren, J. L., Strickland, M. J., Darrow, L. A., & Chang, H. H. (2021). Time-series analysis of daily ambient temperature and emergency department visits in five US cities with a comparison of exposure metrics derived from 1-km meteorology products. *Environ Health*, *20*(1), 1–10. http://dx.doi.org/10.1186/s12940-021-00735-w.

Thornton, P. E., Shrestha, R., Thornton, M., Kao, S.-C., Wei, Y., & Wilson, B. E. (2021). Gridded daily weather data for North America with comprehensive uncertainty quantification. *Science Data*, *8*(1), 190. http://dx.doi.org/10.1038/s41597-021-00973-0.

Van Rossum, G., & Drake, F. (2009). *Documentation for python*, *Python 3 Reference Manual: (Python documentation manual Part 2)*. CreateSpace Independent Publishing Platform, URL https://books.google.ca/books?id=KIybQQAACAAJ.

Vicedo-Cabrera, A. M., Sera, F., & Gasparrini, A. (2019). Hands-on tutorial on a modeling framework for projections of climate change impacts on health. *Epidemiology*, *30*(3), 321. http://dx.doi.org/10.1097/EDE.0000000000000982.

Vimbi, V., Shaffi, N., & Mahmud, M. (2024). Interpreting artificial intelligence models: A systematic review on the application of LIME and SHAP in Alzheimer's disease detection. *Brain Information*, *11*(1), 1–29. http://dx.doi.org/10.1186/s40708-024-00222-1.

Wan, K., Hajat, S., Doherty, R. M., & Feng, Z. (2024). Integrating shared socioeconomic pathway-informed adaptation into temperature-related mortality projections under climate change. *Environmental Research*, *251*, Article 118731. http://dx.doi.org/10.1016/j.envres.2024.118731.

Wang, J. (2023). An intuitive tutorial to Gaussian processes regression. *Computing in Science & Engineering*, 1–8. http://dx.doi.org/10.1109/MCSE.2023.3342149.

Wang, J. J., Katz, J. M., Sanmartin, M. X., Sinvani, L. D., Naidich, J. J., Rula, E. Y., & Sanelli, P. C. (2024). Association between heat vulnerability index and stroke severity. *International Journal of Environmental Research and Public Health*, *21*(8), 1099. http://dx.doi.org/10.3390/ijerph21081099.

Weber, E., Downward, G. S., Ebi, K. L., Lucas, P. L., & van Vuuren, D. (2023). The use of environmental scenarios to project future health effects: A scoping review. *The Lancet Planetary Health*, *7*(7), e611–e621. http://dx.doi.org/10.1016/S2542-5196(23)00110-9.

Weng, Q., Lu, D., & Schubring, J. (2004). Estimation of land surface temperature–Vegetation abundance relationship for urban heat island studies. *Remote Sensing of Environment*, *89*(4), 467–483. http://dx.doi.org/10.1016/j.rse.2003.11.005.

Wood, S. L. R., & Dupras, J. (2021). Increasing functional diversity of the urban canopy for climate resilience: Potential tradeoffs with ecosystem services? *Urban Forestry & Urban Greening*, *58*, Article 126972. http://dx.doi.org/10.1016/j.ufug.2020.126972.

Wu, R., & Wang, B. (2018). Gaussian process regression method for forecasting of mortality rates. *Neurocomputing*, *316*, 232–239. http://dx.doi.org/10.1016/j.neucom.2018.08.001.

Wu, Y., Wen, B., Gasparrini, A., Armstrong, B., Sera, F., Lavigne, E., Li, S., Guo, Y., Overcenco, A., Urban, A. s., Schneider, A., Entezari, A., Vicedo-Cabrera, A. M., Zanobetti, A., Analitis, A., Zeka, A., Tobias, A., Nunes, B., Alahmad, B., ... Guo, Y. (2024). Temperature frequency and mortality: Assessing adaptation to local temperature. *Environment International*, *187*, Article 108691. http://dx.doi.org/10.1016/j.envint.2024.108691.

Xu, Z., Cheng, J., Hu, W., & Tong, S. (2018). Heatwave and health events: A systematic evaluation of different temperature indicators, heatwave intensities and durations. *Science of the Total Environment*, *630*, 679–689. http://dx.doi.org/10.1016/j.scitotenv.2018.02.268.

Yang, Y., Ruan, Z., Wang, X., Yang, Y., Mason, T. G., Lin, H., & Tian, L. (2019). Short-term and long-term exposures to fine particulate matter constituents and health: A systematic review and meta-analysis. *Environmental Pollution*, *247*, 874–882. http://dx.doi.org/10.1016/j.envpol.2018.12.060.

Ye, B., Jiang, J., Liu, J., Zheng, Y., & Zhou, N. (2021). Research on quantitative assessment of climate change risk at an urban scale: Review of recent progress and outlook of future direction. *Renewable and Sustainable Energy Reviews*, *135*, Article 110415. http://dx.doi.org/10.1016/j.rser.2020.110415.

Young, N. E., Anderson, R. S., Chignell, S. M., Vorster, A. G., Lawrence, R., & Evangelista, P. H. (2017). A survival guide to Landsat preprocessing. *Ecology*, *98*(4), 920–932. http://dx.doi.org/10.1002/ecy.1730.

Zakeri, B., Paulavets, K., Barreto-Gomez, L., Echeverri, L. G., Pachauri, S., Boza-Kiss, B., Zimm, C., Rogelj, J., Creutzig, F., Ürge-Vorsatz, D., Victor, D. G., Bazilian, M. D., Fritz, S., Gielen, D., McCollum, D. L., Srivastava, L., Hunt, J. D., & Pouya, S. (2022). Pandemic, war, and global energy transitions. *Energies*, *15*(17), 6114. http://dx.doi.org/10.3390/en15176114.